

Frequency analysis of beams with multiple dampers via exact generalized functions

Giuseppe Failla *

*Department of Civil, Environmental, Energy and Materials Engineering, University of Reggio Calabria
Via Graziella, 89124 Reggio Calabria, Italy*

(Received July 22, 2016, Revised September 22, 2016, Accepted October 5, 2016)

Abstract. This paper deals with frequency analysis of Euler-Bernoulli beams carrying an arbitrary number of Kelvin-Voigt viscoelastic dampers, subjected to harmonic loads. Multiple external/internal dampers occurring at the same position along the beam axis, modeling external damping devices and internal damping due to damage or imperfect connections, are considered. The challenge is to handle simultaneous discontinuities of the response, in particular bending-moment/rotation discontinuities at the location of external/internal rotational dampers, shear-force/deflection discontinuities at the location of external/internal translational dampers. Following a generalized function approach, the paper will show that exact closed-form expressions of the frequency response under point/polynomial loads can readily be derived, for any number of dampers. Also, the exact dynamic stiffness matrix and load vector of the beam will be built in a closed analytical form, to be used in a standard assemblage procedure for exact frequency response analysis of frames.

Keywords: Euler-Bernoulli beam; dynamic Green's function; frequency response function; Kelvin-Voigt viscoelasticity; dampers

1. Introduction

Frequency response analysis of beam-like structures carrying viscoelastic dampers, and subjected to harmonically-varying loads, has been the subject of several studies in the last decades (Housner *et al.* 1997; Soong and Spencer 2002). While frequency response data plays a crucial role for control design, finite element (FE) model updating, system identification or damage detection (Li *et al.* 2014a,b; Keivani *et al.* 2014), beam models with viscoelastic dampers are of interest not only in vibration mitigation applications, but also to model dynamic interaction between beam and coupled sub-systems, or in those cases where flexibility and/or damping arise as a result of damage and imperfections (Ou *et al.* 2007; Kareem and Kline 1995; Sadek *et al.* 1997; Lewandowski and Grzymislawska 2009; Oliveto *et al.* 1997; Xu and Zhang 2001; Kawashima and Fujimoto 1984; Sekulovic *et al.* 2002; Hanss *et al.* 2002; Abdel Raheem 2014). In most studies, a classical Kelvin-Voigt model has been considered as viscoelastic law of dampers.

*Corresponding author, Professor, E-mail: giuseppe.failla@unirc.it

There exist external/internal translational and external/internal rotational dampers.

In frequency response analysis, bending vibrations under harmonic point or distributed loads have been actively investigated, generally within a standard 1D formulation of the equation of motion. In particular, the frequency response to arbitrarily-placed unit point loads provides the so-called dynamic Green's functions (DGFs). DGFs, as well as frequency response functions (FRFs) under distributed loads, can be computed by a classical exact approach. It requires expressing the vibration response over every segment between consecutive positions of dampers/point load, and every segment under a distributed load, in analytical form with 4 integration constants, totaling $4 \times k$ constants for k segments. The integration constants are computed by enforcing matching conditions between the responses over adjacent segments, along with the boundary conditions (B.C.). By this approach, however, the size of the coefficient matrix associated with the set of equations inevitably increases with the number of dampers. Also, it has to be re-inverted numerically for any forcing frequency of interest, and updated whenever dampers or loads change positions. For these reasons, alternative exact or even approximate solutions have been sought. For sake of generality, studies have generally attempted to derive analytical solutions, which may hold for any number of dampers along the beam.

Frequency analysis of bending vibrations has been addressed in several studies. For stepped Euler-Bernoulli (EB) and Timoshenko (TM) beams with an arbitrary number of translational dampers, Sorrentino *et al.* (2003, 2004, 2007) used a transfer matrix approach to derive exact DGFs, based on a direct integration method (Sorrentino *et al.* 2004), or a complex mode superposition with characteristic equation built as determinant of a 4×4 matrix, regardless of the number of dampers (Sorrentino *et al.* 2003; 2007). For a TM beam with an arbitrary number of translational and rotational dampers, Hong and Kim (1999) used a dynamic stiffness matrix method to derive exact DGFs by a complex mode superposition, with characteristic equation built as determinant of a dynamic stiffness matrix whose size, in this case, depends on the number of dampers. For EB beams with an arbitrary number of translational and rotational dampers, Failla (2014; 2016a) used the theory of generalized functions to build exact DGFs and FRFs under polynomial loads, by a direct integration method (Failla 2016a) or complex mode superposition (Failla 2014). The latter extends an approach previously devised by Oliveto *et al.* (1997) for EB beams with end viscous rotational dampers. Approximate yet accurate dynamic Green's functions were built using the eigenfunctions of the bare beam, i.e. the beam without dampers, for an EB beam with an arbitrary number of mass dampers by Wu and Chen (2000), for an EB beam with intermediate viscous translational damper, an intermediate fixed support and a tip mass by Gürgöze and Erol (2002). In frequency analysis of bending vibrations, many other studies have focused on beams carrying an arbitrary number of devices such as external or internal elastic springs, attached masses or spring-mass systems, but without damping. Exact DGFs were derived by the classical approach (Lin 2008, Bambill and Rossit 2002) or using the DGFs of the bare beam on enforcing suitable conditions at locations of supports/masses (Abu-Hilal 2003; Alsaif and Foda 2002; Foda and Albassam 2006) but, in these cases, the number of equations to be solved increases with the number of supports/attachments (Lin 2008; Bambill and Rossit 2002; Abu-Hilal 2003; Alsaif and Foda 2002; Foda and Albassam 2006). For EB beams including an arbitrary number of rotational springs modeling cracks, exact DGFs were obtained by inverting a 8×8 dynamic stiffness matrix built by a transfer matrix method (Khiem and Lien 2002). Further studies on beams with rotational springs modeling cracks have concerned the response to moving loads: for instance, for EB beams a frequency-domain spectral FE method has been proposed by Sarvestan *et al.* (2015), and for TM beams a mode superposition approach involving the modes of the cracked

beam has been pursued by Shafiei and Khaji (2011). The dynamic response of EB beams with end rotational springs has also been studied (Maximov 2014).

Since the combined use of several dampers is resorted to, for instance, for vibration control under different excitation sources (Kareem and Kline 1995; Sadek *et al.* 1997; Lewandowski and Grzymislawska 2009), and in recognition of the fact that dampers may model local damage or imperfect joint and connections (Kawashima and Fujimoto 1984; Sekulovic *et al.* 2002; Hanss *et al.* 2002), there exists an interest in frequency response solutions for beams where multiple dampers may occur simultaneously at the same location: an example could be an external damper, either translational or rotational, applied at a beam section where an internal damper is also introduced to model flexibility/damping due to an imperfect connection or damage. On the other hand, beams with simultaneous occurrence of external supports and internal joints has already been the subject of some studies, focusing on static response. For instance, using the theory of generalized functions Caddemi *et al.* (2013a) derived exact closed-form expressions for the static response of stepped TM beams carrying simultaneous external translational/rotational elastic supports and internal translational/rotational elastic joints. The dynamic response under moving loads of multi-span stepped beams with simultaneous occurrence of external translational/rotational elastic supports and internal translational/rotational elastic joints has been studied by Xu and Li (2008). Computing the dynamic response of beams with multiple dampers requires solving the differential motion equation of the beam coupled with the motion equations of the dampers, with an increasing computational and implementation effort as the number of dampers increases.

Recently, EB beams with multiple external/internal translational and rotational dampers occurring at the same position have been investigated by the author (Failla 2016b). Exact closed-form FRFs have been derived under harmonically-varying point/polynomial loads, for any number of dampers. Specifically, dampers with fractional-derivative constitutive law have been considered. In the same context, the exact dynamic stiffness matrix and load vector of the beam have been derived in a symbolic form, to be assembled for computing the frequency response of 2D frames with multiple dampers. For this purpose, the theory of generalized functions has been used (Yavari *et al.* 2000; Falsone 2002; Caddemi *et al.* 2013a,b; Caddemi *et al.* 2015; Failla and Santini 2007).

This paper revisits the approach devised by the author in his previous study (Failla 2016b), with the aim of presenting a new method to derive an exact analytical form of dynamic stiffness matrix and load vector for beams with an arbitrary number of multiple dampers at the same position, and subjected to harmonically-varying point/polynomial loads. It will be shown that the approach proposed in this paper and the previous one (Failla 2016b) lead to the same exact dynamic stiffness matrix and load vector. However, once the global dynamic stiffness matrix of the frame is built and the nodal displacements are computed, the approach proposed in this paper proves computationally more efficient. In this paper, dampers with Kelvin-Voigt viscoelastic law will be considered.

Upon describing the problem under study in Section 2, Section 3 will present the exact frequency response of the beam with multiple dampers at the same position, under point/polynomial loads. Exact dynamic stiffness matrix and load vector will be presented in Section 4. Numerical applications will be discussed in Section 5.

2. Beams under study

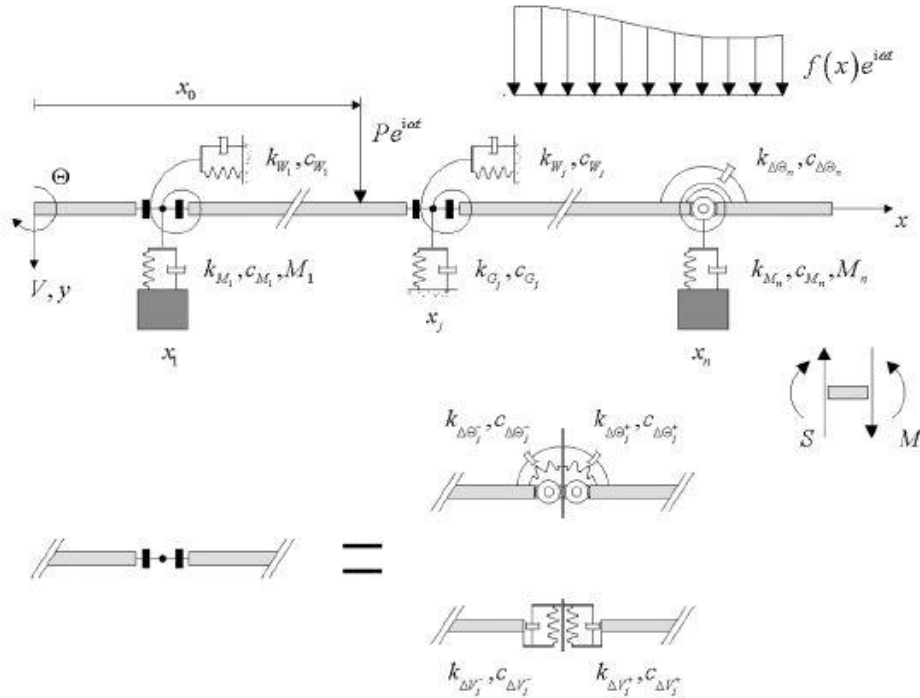


Fig. 1 Euler-Bernoulli beam with multiple Kelvin-Voigt viscoelastic dampers at the same position

Consider the EB beam in Fig. 1. Be x the longitudinal axis, y the transverse axis, L the length, EI the flexural rigidity, m_0 the mass per unit length. Symbols $v(x,t)$, $\theta(x,t)$ denote flexural deflection and bending rotation of the cross section; $s(x,t)$, $m(x,t)$ are shear force, bending moment (Fig. 1 shows positive sign conventions). The beam carries an arbitrary number n of external and internal dampers at abscissas x_j 's along the axis, with Kelvin-Voigt viscoelastic law. For the j th damper, spring stiffness and dash-pot coefficients are indicated below:

- External translational dampers: k_{G_j}, c_{G_j} for grounded dampers; k_{M_j}, c_{M_j} for mass-dampers, with M_j denoting the pertinent mass
- Internal translational dampers: $k_{\Delta V_j^\pm}, c_{\Delta V_j^\pm}$ for right and left dampers
- External rotational dampers: k_{W_j}, c_{W_j}
- Internal rotational dampers: $k_{\Delta\theta_j^\pm}, c_{\Delta\theta_j^\pm}$ for right and left dampers

Equations will be written for the most general case of external and internal dampers occurring simultaneously at the same position. Changes will be straightforward to consider single dampers at a given location, as shown later in the paper.

3. Exact frequency response via generalized function approach

The general framework to build the frequency response of a beam with multiple dampers at the

same position has been outlined by the author in a recent study (Failla 2016b). The fundamental steps are synthesized here for completeness. They will serve as a basis for an original approach to build the exact dynamic stiffness matrix of the beam, in a closed form, as explained in Section 4.

Consider the beam in Fig. 1 loaded by a transverse harmonic load $f(x)e^{i\omega t}$, which acts on the interval (a,b) with $0 \leq a$ and $b \leq L$, and represent the steady-state response variables as $v(x,t)=V(x,\omega)e^{i\omega t}$, $\theta(x,t)=\Theta(x,\omega)e^{i\omega t}$, $s(x,t)=S(x,\omega)e^{i\omega t}$ and $m(x,t)=M(x,\omega)e^{i\omega t}$, the steady-state motion equation is (Wang and Qiao 2007)

$$EI \frac{\bar{d}^4 V(x)}{dx^4} - m_0 \omega^2 V(x) + R(\omega) + \Delta(\omega) + f(x) = 0 \quad (1)$$

where bar means generalized derivative, $R(\omega)$ and $\Delta(\omega)$ are generalized functions given as

$$R(\omega) = - \sum_{j=1}^n R_j(\omega) \delta(x-x_j) + \sum_{j=1}^n W_j(\omega) \delta^{(1)}(x-x_j) \quad (2)$$

$$\Delta(\omega) = - \sum_{j=1}^n EI \cdot \Delta \Theta_j(\omega) \delta^{(2)}(x-x_j) - \sum_{j=1}^n EI \cdot \Delta V_j(\omega) \delta^{(3)}(x-x_j) \quad (3)$$

In Eq.(1), $R_j(\omega)$ and $W_j(\omega)$ are the reactions of the j th external translational damper and external rotational damper, respectively, for which the following relations hold

$$R_j(\omega) + S(x_j^+) = S(x_j^-) \quad (4)$$

$$R_j(\omega) = - \left[\kappa_{G_j}(\omega) + \kappa_{M_j}(\omega) \right] V(x_j) = - \kappa_j(\omega) V(x_j) \quad (5)$$

and

$$W_j(\omega) + M(x_j^-) = M(x_j^+) \quad (6)$$

$$W_j(\omega) = - \kappa_{W_j}(\omega) \Theta(x_j) \quad (7)$$

where $S(x_j^+)$ and $S(x_j^-)$, $M(x_j^+)$ and $M(x_j^-)$ are shear forces and bending moments to the right and left of $x = x_j$. In Eq.(5), $\kappa_{G_j}(\omega)$ and $\kappa_{M_j}(\omega)$ are frequency-dependent terms (Guo and Chen 2007, Wang and Qiao 2007) given as

$$\kappa_{G_j}(\omega) = k_{G_j} + i\omega \cdot c_{G_j}; \quad \kappa_{M_j}(\omega) = \left[\left(k_{M_j} + i\omega \cdot c_{M_j} \right) M_j \omega^2 \right] \left[M_j \omega^2 - \left(k_{M_j} + i\omega \cdot c_{M_j} \right) \right]^{-1} \quad (8a,b)$$

while $\kappa_{W_j}(\omega)$ in Eq.(7) is

$$\kappa_{W_j}(\omega) = k_{W_j} + i\omega \cdot c_{W_j} \quad (9)$$

Eq.(5) is written for the most general case of a grounded and a mass-damper both applied at $x = x_j$. A lumped mass along the beam can be modeled as mass damper with $k_{M_j} = \infty$ in Eq.(8b).

In Eq.(3), $\Delta V_j(\omega)$ and $\Delta \Theta_j(\omega)$ are the relative deflection and rotation between the cross sections at $x = x_j^-$ and $x = x_j^+$, associated with the internal translational and rotational dampers. Based on the constitutive law of the dampers, they are given as

$$\Delta V_j(\omega) = \underbrace{V(x_j^+) - V(x_j)}_{\Delta V_j^+} + \underbrace{V(x_j) - V(x_j^-)}_{\Delta V_j^-} = \frac{S(x_j^+)}{\kappa_{\Delta V_j^+}(\omega)} + \frac{S(x_j^-)}{\kappa_{\Delta V_j^-}(\omega)} \quad (10)$$

$$\Delta \Theta_j(\omega) = \underbrace{\Theta(x_j^+) - \Theta(x_j)}_{\Delta \Theta_j^+} + \underbrace{\Theta(x_j) - \Theta(x_j^-)}_{\Delta \Theta_j^-} = -\frac{M(x_j^+)}{\kappa_{\Delta \Theta_j^+}(\omega)} - \frac{M(x_j^-)}{\kappa_{\Delta \Theta_j^-}(\omega)} \quad (11)$$

where

$$\kappa_{\Delta V_j^\pm}(\omega) = k_{\Delta V_j^\pm} + i\omega \cdot c_{\Delta V_j^\pm} \quad \kappa_{\Delta \Theta_j^\pm}(\omega) = k_{\Delta \Theta_j^\pm} + i\omega \cdot c_{\Delta \Theta_j^\pm} \quad (12)$$

Notice that, in Eq.(1) through Eq.(11), frequency dependence of the response variables $V(x, \omega)$, $\Theta(x, \omega)$, $S(x, \omega)$ and $M(x, \omega)$ is omitted for brevity.

In Eqs.(2)-(3), the reaction force $R_j(\omega)$, reaction moment $W_j(\omega)$, relative deflection $\Delta V_j(\omega)$ and relative rotation $\Delta \Theta_j(\omega)$ at the damper location $x = x_j$ are all unknown. Next, be $\mathbf{Y}(x) = [V(x) \quad \Theta(x) \quad M(x) \quad S(x)]^T$ the vector of frequency response variables solution of Eq.(1), and be $\mathbf{\Lambda}_j = [R_j \quad \Delta V_j \quad W_j \quad \Delta \Theta_j]^T$ the vector collecting the unknown reaction force/moment and relative deflection/rotation at $x = x_j$. Based on the linear superposition principle, $\mathbf{Y}(x)$ can be cast in the general form

$$\mathbf{Y}(x) = \mathbf{\Omega}(x)\mathbf{c} + \sum_{j=1}^n \mathbf{J}(x, x_j)\mathbf{\Lambda}_j + \mathbf{Y}^{(f)}(x) \quad (13)$$

where $\mathbf{\Omega}(x)$ is a 4×4 matrix collecting the response variables derived from the solution of the homogeneous equation associated with Eq.(1), i.e.

$$\mathbf{\Omega}(x)\mathbf{c} = \begin{bmatrix} \Omega_{V1} & \Omega_{V2} & \Omega_{V3} & \Omega_{V4} \\ \Omega_{\Theta1} & \Omega_{\Theta2} & \Omega_{\Theta3} & \Omega_{\Theta4} \\ \Omega_{M1} & \Omega_{M2} & \Omega_{M3} & \Omega_{M4} \\ \Omega_{S1} & \Omega_{S2} & \Omega_{S3} & \Omega_{S4} \end{bmatrix} \begin{bmatrix} c_1 \\ c_2 \\ c_3 \\ c_4 \end{bmatrix} \quad (14)$$

with $\mathbf{c} = [c_1 \ c_2 \ c_3 \ c_4]^T$ vector of integration constants; also, $\mathbf{J}(x, x_j)$ is a 4×4 matrix containing the particular integrals associated with the Dirac's deltas and successive derivatives in Eqs.(1)-(2)-(3), i.e.

$$\mathbf{J}(x, x_j) = \begin{bmatrix} \mathbf{J}^{(P)} & \mathbf{J}^{(\Delta V)} & \mathbf{J}^{(W)} & \mathbf{J}^{(\Delta \Theta)} \end{bmatrix} \quad (15)$$

$$\mathbf{J}^{(P)} = \begin{bmatrix} J_U^{(P)} \\ J_{\Theta}^{(P)} \\ J_M^{(P)} \\ J_S^{(P)} \end{bmatrix}; \quad \mathbf{J}^{(\Delta V)} = \begin{bmatrix} J_U^{(\Delta V)} \\ J_{\Theta}^{(\Delta V)} \\ J_M^{(\Delta V)} \\ J_S^{(\Delta V)} \end{bmatrix}; \quad \mathbf{J}^{(W)} = \begin{bmatrix} J_U^{(W)} \\ J_{\Theta}^{(W)} \\ J_M^{(W)} \\ J_S^{(W)} \end{bmatrix}; \quad \mathbf{J}^{(\Delta \Theta)} = \begin{bmatrix} J_U^{(\Delta \Theta)} \\ J_{\Theta}^{(\Delta \Theta)} \\ J_M^{(\Delta \Theta)} \\ J_S^{(\Delta \Theta)} \end{bmatrix} \quad (16a-d)$$

Specifically, in Eqs.(15)-(16) superscripts (P) , (ΔV) , (W) , $(\Delta \Theta)$ denote respectively the particular integrals associated with a unit transverse force $P=1$, a unit relative deflection $\Delta V=1$, a unit moment $W=1$ and a unit relative rotation $\Delta \Theta=1$, applied at $x = x_j$; finally,

$\mathbf{Y}^{(f)}(x) = [V^{(f)}(x) \ \Theta^{(f)}(x) \ M^{(f)}(x) \ S^{(f)}(x)]^T$ is

$$\mathbf{Y}^{(f)}(x) = \int_a^b \mathbf{J}^{(P)}(x, \xi) f(\xi) d\xi \quad (17)$$

All terms in Eqs.(14)-(15) are available in a simple analytical form, which involve typical generalized functions. Closed-form solutions are available also for Eq.(17) related to the applied load, following simple rules of integration of generalized functions. For brevity, pertinent equations are reported in Appendix A.

Based on Eqs.(5)-(7) and Eqs.(10)-(11), the unknowns Λ_j can be expressed in terms of the integration constants \mathbf{c} , yielding the following general form of the FRFs

$$\mathbf{Y}(x) = \tilde{\mathbf{Y}}(x)\mathbf{c} + \tilde{\mathbf{Y}}^{(f)}(x) \quad (18)$$

where $\tilde{\mathbf{Y}}(x)$ and $\tilde{\mathbf{Y}}^{(f)}(x)$ are given as

$$\tilde{\mathbf{Y}}(x) = \mathbf{\Omega}(x) + \sum_{j=1}^n \mathbf{J}(x, x_j) \mathbf{\Phi}_{\Omega}(x_j) + \sum_{j=2}^n \mathbf{J}(x, x_j) \left\{ \sum_{(j,l) \in \square_2^{(j)}} \mathbf{\Phi}_{\mathbf{J}}(x_j^-, x_l) \mathbf{\Phi}_{\Omega}(x_l) + \right. \\ \left. \sum_{2 < q \leq j} \sum_{\substack{(j,l,m,\dots,r,s) \in \square_q^{(j)} \\ q}} \mathbf{\Phi}_{\mathbf{J}}(x_j^-, x_l) \mathbf{\Phi}_{\mathbf{J}}(x_l^-, x_m) \cdots \mathbf{\Phi}_{\mathbf{J}}(x_r^-, x_s) \mathbf{\Phi}_{\Omega}(x_s) \right\} \quad (19)$$

$$\tilde{\mathbf{Y}}^{(f)}(x) = \mathbf{Y}^{(f)}(x) + \sum_{j=1}^n \mathbf{J}(x, x_j) \mathbf{\Phi}^{(f)}(x_j) + \sum_{j=2}^n \mathbf{J}(x, x_j) \left\{ \sum_{(j,l) \in \square_2^{(j)}} \mathbf{\Phi}_{\mathbf{J}}(x_j^-, x_l) \mathbf{\Phi}^{(f)}(x_l) + \right. \\ \left. \sum_{2 < q \leq j} \sum_{\substack{(j,l,m,\dots,r,s) \in \square_q^{(j)} \\ q}} \mathbf{\Phi}_{\mathbf{J}}(x_j^-, x_l) \mathbf{\Phi}_{\mathbf{J}}(x_l^-, x_m) \cdots \mathbf{\Phi}_{\mathbf{J}}(x_r^-, x_s) \mathbf{\Phi}^{(f)}(x_s) \right\} \quad (20)$$

where $\square_q^{(j)} = \{ \underbrace{(j, l, m, \dots, r, s)}_q : j > l > m > \dots > r > s; l, m, \dots, r, s = 1, 2, \dots, (j-1) \}$ is the set including all possible q -ples of indexes $\underbrace{(j, l, m, \dots, r, s)}_q$ such that $j > l > m > \dots > r > s$, being $2 \leq q \leq j$. In Eq.(19), symbol $\mathbf{\Phi}_{\Omega}(x_j)$ denotes the 4×4 matrix

$$\mathbf{\Phi}_{\Omega}(x_j) = \begin{bmatrix} -\kappa_j(\omega) \left((\mathbf{\Omega}(x_j))_1 + \frac{(\mathbf{\Omega}(x_j))_4}{\kappa_{\Delta V_j^-}(\omega)} \right) \\ \left(\frac{1}{\kappa_{\Delta V_j^-}(\omega)} + \frac{1}{\kappa_{\Delta V_j^+}(\omega)} \right) (\mathbf{\Omega}(x_j))_4 + \frac{\kappa_j(\omega)}{\kappa_{\Delta V_j^+}(\omega)} \left((\mathbf{\Omega}(x_j))_1 + \frac{(\mathbf{\Omega}(x_j))_4}{\kappa_{\Delta V_j^-}(\omega)} \right) \\ -\kappa_{W_j}(\omega) \left((\mathbf{\Omega}(x_j))_2 - \frac{(\mathbf{\Omega}(x_j))_3}{\kappa_{\Delta \Theta_j^-}(\omega)} \right) \\ - \left(\frac{1}{\kappa_{\Delta \Theta_j^-}(\omega)} + \frac{1}{\kappa_{\Delta \Theta_j^+}(\omega)} \right) (\mathbf{\Omega}(x_j))_3 + \frac{\kappa_{W_j}(\omega)}{\kappa_{\Delta \Theta_j^+}(\omega)} \left((\mathbf{\Omega}(x_j))_2 - \frac{(\mathbf{\Omega}(x_j))_3}{\kappa_{\Delta \Theta_j^-}(\omega)} \right) \end{bmatrix} \quad (21)$$

being $(\mathbf{\Omega}(x_j))_i$ row vectors coinciding with the i th row of matrix $\mathbf{\Omega}(x_j)$. Further, for $k < j$, $\mathbf{\Phi}_J(x_j^-, x_k)$ is the 4×4 matrix

$$\mathbf{\Phi}_J(x_j^-, x_k) = \begin{bmatrix} -\kappa_j(\omega) \left((\mathbf{J}(x_j^-, x_k))_1 + \frac{(\mathbf{J}(x_j^-, x_k))_4}{\kappa_{\Delta V_j^-}(\omega)} \right) \\ \left(\frac{1}{\kappa_{\Delta V_j^-}(\omega)} + \frac{1}{\kappa_{\Delta V_j^+}(\omega)} \right) (\mathbf{J}(x_j^-, x_k))_4 + \frac{\kappa_j(\omega)}{\kappa_{\Delta V_j^+}(\omega)} \left((\mathbf{J}(x_j^-, x_k))_1 + \frac{(\mathbf{J}(x_j^-, x_k))_4}{\kappa_{\Delta V_j^-}(\omega)} \right) \\ -\kappa_{W_j}(\omega) \left((\mathbf{J}(x_j^-, x_k))_2 - \frac{(\mathbf{J}(x_j^-, x_k))_3}{\kappa_{\Delta \Theta_j^-}(\omega)} \right) \\ - \left(\frac{1}{\kappa_{\Delta \Theta_j^-}(\omega)} + \frac{1}{\kappa_{\Delta \Theta_j^+}(\omega)} \right) (\mathbf{J}(x_j^-, x_k))_3 + \frac{\kappa_{W_j}(\omega)}{\kappa_{\Delta \Theta_j^+}(\omega)} \left((\mathbf{J}(x_j^-, x_k))_2 - \frac{(\mathbf{J}(x_j^-, x_k))_3}{\kappa_{\Delta \Theta_j^-}(\omega)} \right) \end{bmatrix} \quad (22)$$

where $(\mathbf{J}(x_j^-, x_k))_i$ are the row vectors coinciding with the i th row of matrix $\mathbf{J}(x_j^-, x_k)$, and $\mathbf{\Phi}^{(f)}(x_j)$ is the 4×1 vector

$$\mathbf{\Phi}^{(f)}(x_j) = \begin{bmatrix} -\kappa_j(\omega) \left(\mathbf{V}^{(f)}(x_j) + \frac{\mathbf{S}^{(f)}(x_j)}{\kappa_{\Delta V_j^-}(\omega)} \right) \\ \left(\frac{1}{\kappa_{\Delta V_j^-}(\omega)} + \frac{1}{\kappa_{\Delta V_j^+}(\omega)} \right) \mathbf{S}^{(f)}(x_j) + \frac{\kappa_j(\omega)}{\kappa_{\Delta V_j^+}(\omega)} \left(\mathbf{V}^{(f)}(x_j) + \frac{\mathbf{S}^{(f)}(x_j)}{\kappa_{\Delta V_j^-}(\omega)} \right) \\ -\kappa_{W_j}(\omega) \left(\mathbf{\Theta}^{(f)}(x_j) - \frac{\mathbf{M}^{(f)}(x_j)}{\kappa_{\Delta \Theta_j^-}(\omega)} \right) \\ - \left(\frac{1}{\kappa_{\Delta \Theta_j^-}(\omega)} + \frac{1}{\kappa_{\Delta \Theta_j^+}(\omega)} \right) \mathbf{M}^{(f)}(x_j) + \frac{\kappa_{W_j}(\omega)}{\kappa_{\Delta \Theta_j^+}(\omega)} \left(\mathbf{\Theta}^{(f)}(x_j) - \frac{\mathbf{M}^{(f)}(x_j)}{\kappa_{\Delta \Theta_j^-}(\omega)} \right) \end{bmatrix} \quad (23)$$

All terms in Eqs.(21)-(23) are given in Appendix A, for brevity.

At this stage, the integration constants \mathbf{c} in Eq. (18) can be computed by enforcing the B.C. of the beam. This leads to 4 equations, regardless of the number of dampers, with general form

$$\mathbf{Bc} = \mathbf{r} \quad \rightarrow \quad \mathbf{c} = \mathbf{B}^{-1} \mathbf{r} \quad (24)$$

where vector \mathbf{r} involves the load-dependent terms $\tilde{\mathbf{Y}}^{(f)}(x)$ in Eq.(18), as computed at the beam ends. Due to the limited size (4×4), the coefficient matrix \mathbf{B} can readily be inverted in a symbolic form (e.g., see Failla (2016a)). Therefore, upon deriving \mathbf{c} from Eq.(24), Eq.(18) provides exact closed-form expressions for the frequency response vector $\mathbf{Y}(x)$. The load-dependent term $\mathbf{Y}^{(f)}(x)$ can be solved in a closed form for any loading function $f(x)$ for which a primitive exists as, for instance, polynomial loads (see Appendix A).

3.1 Remarks

Eq.(18) can be used for both homogeneous and non-homogeneous B.C., the latter as due to end dampers. In this case homogeneous B.C. can still be considered, while the end dampers are modelled as internal dampers located at $x_1 = 0^+$ and $x_n = L^-$ (Failla 2016a).

Eq.(18) for $\mathbf{Y}(x)$ have been derived for the most general case of multiple dampers occurring simultaneously at the same location $x = x_j$. Changes for single dampers occurring at a given location are immediate, as explained in the following.

If no external translational damper occurs at $x = x_j$, $\kappa_j(\omega) = 0$ shall be set at $x = x_j$. This will automatically set equal to zero the 1st row in matrices $\Phi_\Omega(x_j)$, $\Phi_J(x_j^-, x_k)$ and $\Phi^{(f)}(x_j)$. In addition, being $R_j = 0$ at $x = x_j$, the 1st column of matrix $\Phi_J(x_m^-, x_j)$ shall be set equal to zero for all $x_m^- > x_j$. Obviously, if at $x = x_j$ there is no external translational damper but there is an internal translational damper, $S(x_j^-) = S(x_j^+)$ and, in view of Eq.(10), $\kappa_{\Delta V_j^+}(\omega) = \kappa_{\Delta V_j^-}(\omega) = \kappa_{\Delta V_j}(\omega)/2$, with $\kappa_{\Delta V_j}(\omega)$ frequency-dependent stiffness of the internal translational damper at $x = x_j$.

If no internal translational damper occurs at $x = x_j$, $\kappa_{\Delta V_j^+}(\omega) = \kappa_{\Delta V_j^-}(\omega) = \infty$ shall be set at $x = x_j$. As a result, the 2nd row of matrices $\Phi_\Omega(x_j)$, $\Phi_J(x_j^-, x_k)$ and $\Phi^{(f)}(x_j)$ will be equal to zero. Also, being $\Delta V_j = 0$ at $x = x_j$, the 2nd column of matrix $\Phi_J(x_m^-, x_j)$ shall be set equal to zero for all $x_m^- > x_j$.

Changes to be made if no external rotational damper or internal rotational damper occurs at $x = x_j$ mirror those explained above for the translational dampers, and are not reported for brevity (if only an internal rotational damper occurs at $x = x_j$, its frequency-dependent stiffness will be denoted as $\kappa_{\Delta \theta_j}(\omega)$, with $M(x_j^-) = M(x_j^+)$ and $\kappa_{\Delta \theta_j^+}(\omega) = \kappa_{\Delta \theta_j^-}(\omega) = \kappa_{\Delta \theta_j}(\omega)/2$ in Eq.(11), see Fig. 1).

It is noticed that Eq.(18) has been derived for distributed load $f(x)$. If the applied load is a point force, i.e. $f(x) = P \cdot \delta(x - x_0)$ at $x = x_0$, Eq.(17) yields $\mathbf{Y}^{(f)}(x) = P \cdot \mathbf{J}^{(P)}(x, x_0)$. Whereas the point force $P \cdot \delta(x - x_0)$ is applied at a damper location $x = x_j$, i.e. $x_0 = x_j$, Eq.(4) will be written as

$R_j(\omega) + P + S(x_j^+) = S(x_j^-)$. Consequently, an additional term $-P/\kappa_{\Delta V_j^+}(\omega)$ shall be considered on the r.h.s. of Eq.(10) and in the 2nd entry of vector $\Phi^{(f)}(x_j)$ given by Eq.(23) where, in this case, $S^{(f)}(x)$ will be computed at $x = x_j^-$ (unlike the case of distributed load $f(x)$, the shear force $S^{(f)}(x)$ is now discontinuous at $x = x_j$ since the point force is applied at $x = x_0$).

Final remarks concern the computational advantages of the proposed approach. Eq.(18) is an exact closed-form expression of the FRFs, fulfilling all required conditions at the locations of dampers and point load (see Appendix A). On the contrary, by the classical exact approach the vibration response in every beam segment, either between two consecutive positions of dampers/point load or under a distributed load, must be represented in terms of 4 integration constants, totaling $4 \times k$ constants for k segments, to be computed by a set of equations built from the B.C. and matching conditions between the responses over contiguous segments. Obviously, by this approach the coefficient matrix associated with the set of equations to be solved has to be updated whenever positions of dampers or loads change along the beam axis, and its size increases with the number of dampers. Also, it has to be re-inverted for any forcing frequency of the applied load. Eq.(18) can also serve as benchmark for FRFs built by a standard FE method with two-node beam elements. Further advantages are that, in a standard FE method, a mesh node shall be inserted at the application point of any damper or point load, and re-meshing may be required whenever dampers or load change position.

4. Dynamic stiffness matrix and load vector

Consider the beam in Fig. 1 as a beam element with two nodes at the ends. Each node has three degrees of freedom. Let $\mathbf{u} = [U_1 \ V_1 \ \Theta_1 \ U_2 \ V_2 \ \Theta_2]^T$ be the vector collecting nodal displacements: $U_1 = U(0)$ and $U_2 = U(L)$ with $U(x)$ axial displacement positive rightward; $V_1 = V(0)$ and $V_2 = V(L)$ with $V(x)$ transverse displacement positive downward; $\Theta_1 = \Theta(0)$ and $\Theta_2 = \Theta(L)$ with $\Theta(x)$ rotation positive clockwise. Correspondingly, be $\mathbf{f} = [H_1 \ Q_1 \ C_1 \ H_2 \ Q_2 \ C_2]^T$ the vector collecting nodal forces that, in view of the positive sign conventions for nodal forces and internal stress resultants, read

$$\begin{aligned}
 H_1 &= -N(0) & Q_1 &= -S(0) & C_1 &= M(0) \\
 H_2 &= N(L) & Q_2 &= S(L) & C_2 &= -M(L)
 \end{aligned} \tag{25}$$

where $N(x)$ is the axial force, $S(x)$ is the shear force and $M(x)$ the bending moment. The following nodal relation holds

$$\mathbf{f} = \mathbf{D}(\omega)\mathbf{u} + \mathbf{f}_0 \tag{26}$$

where $\mathbf{D}(\omega)$ is the dynamic stiffness matrix, \mathbf{f}_0 is the nodal force vector attributable to the loads acting along the beam. It will be shown that elements of both matrix $\mathbf{D}(\omega)$ and vector \mathbf{f}_0 can be derived based on the frequency response (18), on assuming that both ends are clamped.

4.1 Exact dynamic stiffness matrix

Be $\mathbf{G}^{(r)}(x, x_0) = [V^{(r)} \quad \Theta^{(r)} \quad M^{(r)} \quad S^{(r)}]^T$, for $r = V, \Theta$, the frequency response vector of the clamped-clamped beam, subjected to a harmonic unit deflection $V \cdot e^{i\omega t}$, $V=1$, and harmonic unit rotation $\Theta \cdot e^{i\omega t}$, $\Theta=1$, applied at the beam ends $x_0 = 0$ or $x_0 = L$. It is noted that $\mathbf{G}^{(r)}(x, x_0)$ takes the form (18) with no load-dependent terms $\tilde{\mathbf{Y}}^{(f)}(x)$, i.e.

$$\mathbf{G}^{(r)}(x, x_0) = \tilde{\mathbf{Y}}(x) \mathbf{e}^{(r)} \quad \text{for } \mathbf{e}^{(r)} = \mathbf{B}^{-1} \mathbf{e}^{(r)} \quad r = V, \Theta \quad (27)$$

In Eq.(27), matrix \mathbf{B} is

$$\mathbf{B} = \begin{bmatrix} (\tilde{\mathbf{Y}}(0))_{1,1} & (\tilde{\mathbf{Y}}(0))_{1,2} & (\tilde{\mathbf{Y}}(0))_{1,3} & (\tilde{\mathbf{Y}}(0))_{1,4} \\ (\tilde{\mathbf{Y}}(0))_{2,1} & (\tilde{\mathbf{Y}}(0))_{2,2} & (\tilde{\mathbf{Y}}(0))_{2,3} & (\tilde{\mathbf{Y}}(0))_{2,4} \\ (\tilde{\mathbf{Y}}(L))_{1,1} & (\tilde{\mathbf{Y}}(L))_{1,2} & (\tilde{\mathbf{Y}}(L))_{1,3} & (\tilde{\mathbf{Y}}(L))_{1,4} \\ (\tilde{\mathbf{Y}}(L))_{2,1} & (\tilde{\mathbf{Y}}(L))_{2,2} & (\tilde{\mathbf{Y}}(L))_{2,3} & (\tilde{\mathbf{Y}}(L))_{2,4} \end{bmatrix} \quad (28)$$

where $(\tilde{\mathbf{Y}})_{m,n}(\cdot)$ denotes the m,n element of matrix $\tilde{\mathbf{Y}}(x)$ given by Eq.(19), while vectors $\mathbf{e}^{(r)}$ are given as

$$\mathbf{e}^{(V)} = [1 \quad 0 \quad 0 \quad 0]^T \quad \text{if } x_0 = 0 \quad (29)$$

$$\mathbf{e}^{(V)} = [0 \quad 0 \quad 1 \quad 0]^T \quad \text{if } x_0 = L$$

$$\mathbf{e}^{(\Theta)} = [0 \quad 1 \quad 0 \quad 0]^T \quad \text{if } x_0 = 0$$

$$\mathbf{e}^{(\Theta)} = [0 \quad 0 \quad 0 \quad 1]^T \quad \text{if } x_0 = L \quad (30)$$

At this stage, the elements of matrix $\mathbf{D}(\omega)$ can be built based on the Eq.(27). In particular, bearing in mind that the elements of the dynamic stiffness matrix $\mathbf{D}(\omega)$ are the nodal forces due to unit displacements/rotations at the nodes, and taking into account the relations (25) between nodal

forces and stress resultants, it yields

$$\mathbf{D}(\omega) = \begin{bmatrix} -N^{(U)}(0,0) & 0 & 0 & -N^{(U)}(0,L) & 0 & 0 \\ 0 & -S^{(V)}(0,0) & -S^{(\Theta)}(0,0) & 0 & -S^{(V)}(0,L) & -S^{(\Theta)}(0,L) \\ 0 & M^{(V)}(0,0) & M^{(\Theta)}(0,0) & 0 & M^{(V)}(0,L) & M^{(\Theta)}(0,L) \\ N^{(U)}(L,0) & 0 & 0 & N^{(U)}(L,L) & 0 & 0 \\ 0 & S^{(V)}(L,0) & S^{(\Theta)}(L,0) & 0 & S^{(V)}(L,L) & S^{(\Theta)}(L,L) \\ 0 & -M^{(V)}(L,0) & -M^{(\Theta)}(L,0) & 0 & -M^{(V)}(L,L) & -M^{(\Theta)}(L,L) \end{bmatrix} \quad (31)$$

where $S^{(r)}(x, x_0)$ and $M^{(r)}(x, x_0)$ for $r = V, \Theta$, are given by Eq.(27) with $x = 0, L$ and $x_0 = 0, L$. It is worth remarking that all elements in Eq.(31) for $\mathbf{D}(\omega)$ are readily available in a closed form, as Eq.(27) are closed-form expressions for $\mathbf{G}^{(V)}(x, x_0)$ and $\mathbf{G}^{(\Theta)}(x, x_0)$, as explained in Section 3. Also, $N^{(U)}(x, x_0)$ is obtained from the steady-state axial vibration equation

$$EA \frac{d^2 U(x)}{dx^2} + m_0 \omega^2 U(x) = 0 \quad (32)$$

under harmonic unit axial displacements $U \cdot e^{i\omega t}$, $U = 1$, applied at the beam ends $x_0 = 0$ or $x_0 = L$. Bearing in mind that the solution to Eq.(30) is

$$U(x) = a_1 U_{11}(x) + a_2 U_{12}(x) = a_1 \cos(\eta x) + a_2 \sin(\eta x) \quad (33)$$

with corresponding axial force

$$N(x) = EA \frac{dU}{dx} = a_1 N_{11}(x) + a_2 N_{12}(x) = -a_1 \eta \sin(\eta x) + a_2 \eta \cos(\eta x) \quad (34)$$

for $\eta = \eta(\omega) = EA^{-1/2} m_0^{1/2} \omega$, terms $N^{(U)}(x, 0)$ and $N^{(U)}(x, L)$ in Eq.(31), for $x = 0$ and $x = L$, can readily be obtained from Eq.(34) on computing the two sets of integration constants (a_1, a_2) corresponding, respectively, to the following boundary conditions: $U(0) = 1, U(L) = 0$; and $U(0) = 0, U(L) = 1$.

4.2 Exact load vector

Next, denote by $\mathbf{Y}_0(x) = [V_0 \quad \Theta_0 \quad M_0 \quad S_0]^T$ the frequency response vector (18) of the beam in Fig. 1 under loads $f(x)$, when both ends of the beam are clamped. Be $\mathbf{c}^{(f)}$ the vector of

integration constants in Eq.(18) where, in this case, superscript (f) distinguishes vector $\mathbf{c}^{(f)}$ from vectors $\mathbf{c}^{(v)}$ and $\mathbf{c}^{(\theta)}$ associated with unit deflection and rotation at the beam ends, see Eq.(27). They are computed by the following equations

$$\mathbf{B}\mathbf{c}^{(f)} = \mathbf{e}^{(f)} \quad \mathbf{e}^{(f)} = -\left[\tilde{v}^{(f)}(0) \quad \tilde{\theta}^{(f)}(0) \quad \tilde{v}^{(f)}(L) \quad \tilde{\theta}^{(f)}(L)\right]^T \quad (35)$$

Using the closed-form expressions (18), and in view of relations (25), the exact load vector is then given in the closed form

$$\mathbf{f}_0 = \left[0 \quad -S_0(0) \quad M_0(0) \quad 0 \quad S_0(L) \quad -M_0(L)\right]^T \quad (36)$$

In Eq.(36), it is assumed that no harmonic axial loads act along the beam, although pertinent terms could readily be obtained from steady-state equations (32) under axial load.

Now, exact dynamic stiffness matrix and load vector can be assembled by a standard FE procedure. It is interesting to note that dynamic stiffness matrix and load vector hold the same size, i.e. 6×6 and 6×1 , for any number of dampers and loads. For this, the size of the corresponding global matrix and vector will depend only on the number of beam-to-column nodes, regardless of the number of dampers and loads.

Upon deriving the global node solution, the exact frequency response can be built in every frame member, using the following general expression

$$\mathbf{Y}(x) = \mathbf{G}^{(v)}(x,0)V_1 + \mathbf{G}^{(\theta)}(x,0)\Theta_1 + \mathbf{G}^{(v)}(x,L)V_2 + \mathbf{G}^{(\theta)}(x,L)\Theta_2 + \mathbf{Y}_0(x) \quad (37)$$

where V_i and Θ_i are the nodal displacements in vector \mathbf{u} , while represent the frequency response of the clamped-clamped beam to the applied loads.

At this stage, a few remarks are in order. The exact dynamic stiffness matrix (31) and load vector (36) can be derived by an alternative procedure, proposed in a previous study (Failla 2016b) and briefly recalled in Appendix B. Although the two approaches lead both to the exact dynamic stiffness matrix and load vector in a symbolic form, there is a relevant difference between the two approaches. Once the global dynamic stiffness matrix of the frame is built and the nodal displacements \mathbf{u} are computed, the previous approach (Failla, 2016b) requires back-calculating the vector of integration constants $\mathbf{b} = [a_1 \quad a_2 \quad c_1 \quad c_2 \quad c_3 \quad c_4]^T$ in Eq.(B.8); the latter includes indeed vector $\mathbf{c} = [c_1 \quad c_2 \quad c_3 \quad c_4]^T$, to be used in Eq.(18) to compute the frequency response vector along the beam. On the contrary, Eq.(37) is expressed directly in terms of nodal displacements \mathbf{u} . This provides an immediate insight into how the response variables along the beam are affected by nodal displacements and loads, with relevant advantages in terms of computational effort.

5. Numerical application

Consider the beam in Fig. 2 with parameters: $L=15$ m, $EI=1.055 \times 10^7$ Nm², $m_0=49.54$ kgm⁻¹ (corresponding to a Young's modulus = 19.5×10^{10} Nm⁻²; moment of inertia 5.41×10^{-5} m⁴; cross section area = 64.34×10^{-4} m²; mass density = 7.7×10^3 kgm⁻³). Two external translational dampers

and two external rotational dampers are applied at $x = L/3$ and $x = 2L/3$. Also, it is assumed that internal translational and rotational dampers are located to the right and left of $x = L/3$ and $x = 2L/3$, modeling imperfect/damaged connections. Parameters are given in Table 1.

Free and forced vibrations are investigated under various loading conditions, using exact proposed method and exact classical method. The first makes use of the closed-form expression (18), with a total number of $n=2$ damper locations, i.e. $\square_2^{(2)} = \{(2,1)\}$ only is considered in Eq.(18).

The second involves $4 \times 4 = 16$ integration constants for the frequency response to a point load at $x_0 \neq x_1, x_2$ (i.e. not occurring at damper locations) and $4 \times 5 = 20$ for the frequency response to the distributed loads over $[L/6, L/2]$, to be computed by inverting the coefficient matrix associated with the matching conditions + 4 B.C. (the steady-state response over each segment between two consecutive damper/point load locations or under distributed load is represented in terms of 4 integration constants). For the beam segment under the uniform or linear load, a particular integral can readily be obtained in a closed form by Mathematica (Wolfram, 2008). Due to the large size, in this case matrix inversion is performed numerically, and the inverse matrix shall be re-computed for any forcing frequency of interest. Analogous comments hold when free vibration responses are built by both proposed and classical method. By the proposed method, exact eigenvalues are built as root of the transcendental equation $\det(\mathbf{B})=0$, where \mathbf{B} is the 4×4 matrix in Eq.(24).

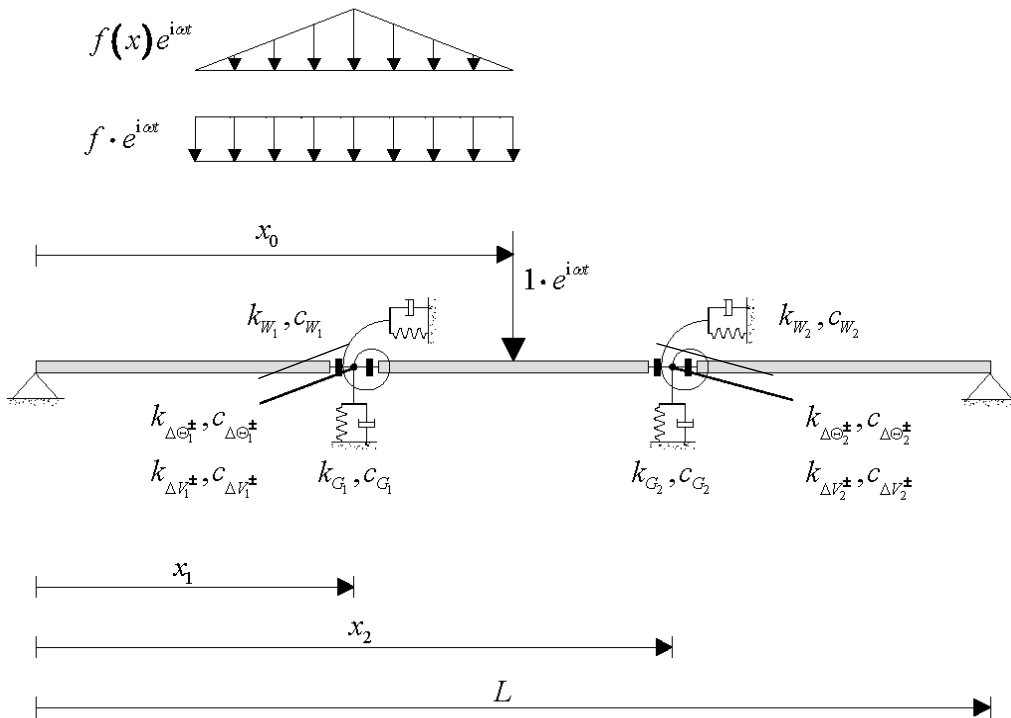


Fig. 2 Beam with multiple dampers at $x_1=L/3$ and $x_2=2L/3$, under: (a) point load $1 \times e^{i\omega t}$ at $x=x_0$; (b) uniform load $f \times e^{i\omega t}$ over $[L/6, L/2]$, with $f=3/a \text{ Nm}^{-1}$ for $a=15$; (c) linear load $f(x) \times e^{i\omega t}$, with $f(x)=36(x-a/6)/a^2 \text{ Nm}^{-1}$ over $[L/6, L/3]$, $f(x) = 36(a/2-x)/a^2 \text{ Nm}^{-1}$ over $[L/3, L/2]$ for $a=15$.

Table 1 Beam in Fig. 2: spring stiffness and damping coefficients of dampers

Damper	Spring stiffness	Damping coefficient
Ext. translational damper at $x_1 = L/3$	$k_{G_1} = 3.13 \times 10^5 \text{ Nm}^{-1}$	$c_{G_1} = 1.52 \times 10^3 \text{ Nm}^{-1}\text{s}$
Int. translational damper at $x_1^- = (L/3)^-$	$k_{\Delta V_1^-} = 1.56 \times 10^8 \text{ Nm}^{-1}$	$c_{\Delta V_1^-} = 1.52 \times 10^3 \text{ Nm}^{-1}\text{s}$
Int. translational damper at $x_1^+ = (L/3)^+$	$k_{\Delta V_1^+} = 1.56 \times 10^8 \text{ Nm}^{-1}$	$c_{\Delta V_1^+} = 1.52 \times 10^3 \text{ Nm}^{-1}\text{s}$
Ext. rotational damper at $x_1 = L/3$	$k_{W_1} = 3.43 \times 10^5 \text{ Nm}$	$c_{W_1} = 7.03 \times 10^8 \text{ Nms}$
Int. rotational damper at $x_1^- = (L/3)^-$	$k_{\Delta \Theta_1^-} = 7.03 \times 10^6 \text{ Nm}$	$c_{\Delta \Theta_1^-} = 3.43 \times 10^5 \text{ Nms}$
Int. rotational damper at $x_1^+ = (L/3)^+$	$k_{\Delta \Theta_1^+} = 7.03 \times 10^6 \text{ Nm}$	$c_{\Delta \Theta_1^+} = 3.43 \times 10^5 \text{ Nms}$
Ext. translational damper at $x_2 = 2L/3$	$k_{G_2} = 3.13 \times 10^5 \text{ Nm}^{-1}$	$c_{G_2} = 1.52 \times 10^3 \text{ Nm}^{-1}\text{s}$
Int. translational damper at $x_2^- = (2L/3)^-$	$k_{\Delta V_2^-} = 1.56 \times 10^8 \text{ Nm}^{-1}$	$c_{\Delta V_2^-} = 1.52 \times 10^3 \text{ Nm}^{-1}\text{s}$
Int. translational damper at $x_2^+ = (2L/3)^+$	$k_{\Delta V_2^+} = 1.56 \times 10^8 \text{ Nm}^{-1}$	$c_{\Delta V_2^+} = 1.52 \times 10^3 \text{ Nm}^{-1}\text{s}$
Ext. rotational damper at $x_2 = 2L/3$	$k_{W_2} = 3.43 \times 10^5 \text{ Nm}$	$c_{W_2} = 7.03 \times 10^8 \text{ Nms}$
Int. rotational damper at $x_2^- = (2L/3)^-$	$k_{\Delta \Theta_2^-} = 7.03 \times 10^6 \text{ Nm}$	$c_{\Delta \Theta_2^-} = 3.43 \times 10^5 \text{ Nms}$
Int. rotational damper at $x_2^+ = (2L/3)^+$	$k_{\Delta \Theta_2^+} = 7.03 \times 10^6 \text{ Nm}$	$c_{\Delta \Theta_2^+} = 3.43 \times 10^5 \text{ Nms}$

Figs. 3-4 show the deflection eigenfunctions of the first 4 modes. Corresponding eigenvalues are reported in Table 2, along with the damping ratio = $\text{Im}(\text{Eigenvalue})/\text{Abs}(\text{Eigenvalue})$. The agreement between proposed and classical solutions is excellent. It is noticed that the deflection is discontinuous due to the presence of the internal translational dampers. Figs. 3-4 report the deflections at $x = x_1^\pm$ and $x = x_2^\pm$; from these, the deflection at the application points of the external translational dampers, i.e. at $x = x_1$ and $x = x_2$, can readily be derived using

$$V(x_j^+) - V(x_j) = \frac{S(x_j^+)}{\kappa_{\Delta V_j^+}(\omega)} \rightarrow V(x_j) = V(x_j^+) - \frac{S(x_j^+)}{\kappa_{\Delta V_j^+}(\omega)} \quad (38)$$

Obviously, a similar expression could be used to derive the rotation at the application point of the external rotational dampers from the rotations at $x = x_1^\pm$ and $x = x_2^\pm$, here reported for later convenience

$$\Theta(x_j^+) - \Theta(x_j) = -\frac{M(x_j^+)}{\kappa_{\Delta \Theta_j^+}(\omega)} \rightarrow \Theta(x_j) = \Theta(x_j^+) + \frac{M(x_j^+)}{\kappa_{\Delta \Theta_j^+}(\omega)} \quad (39)$$

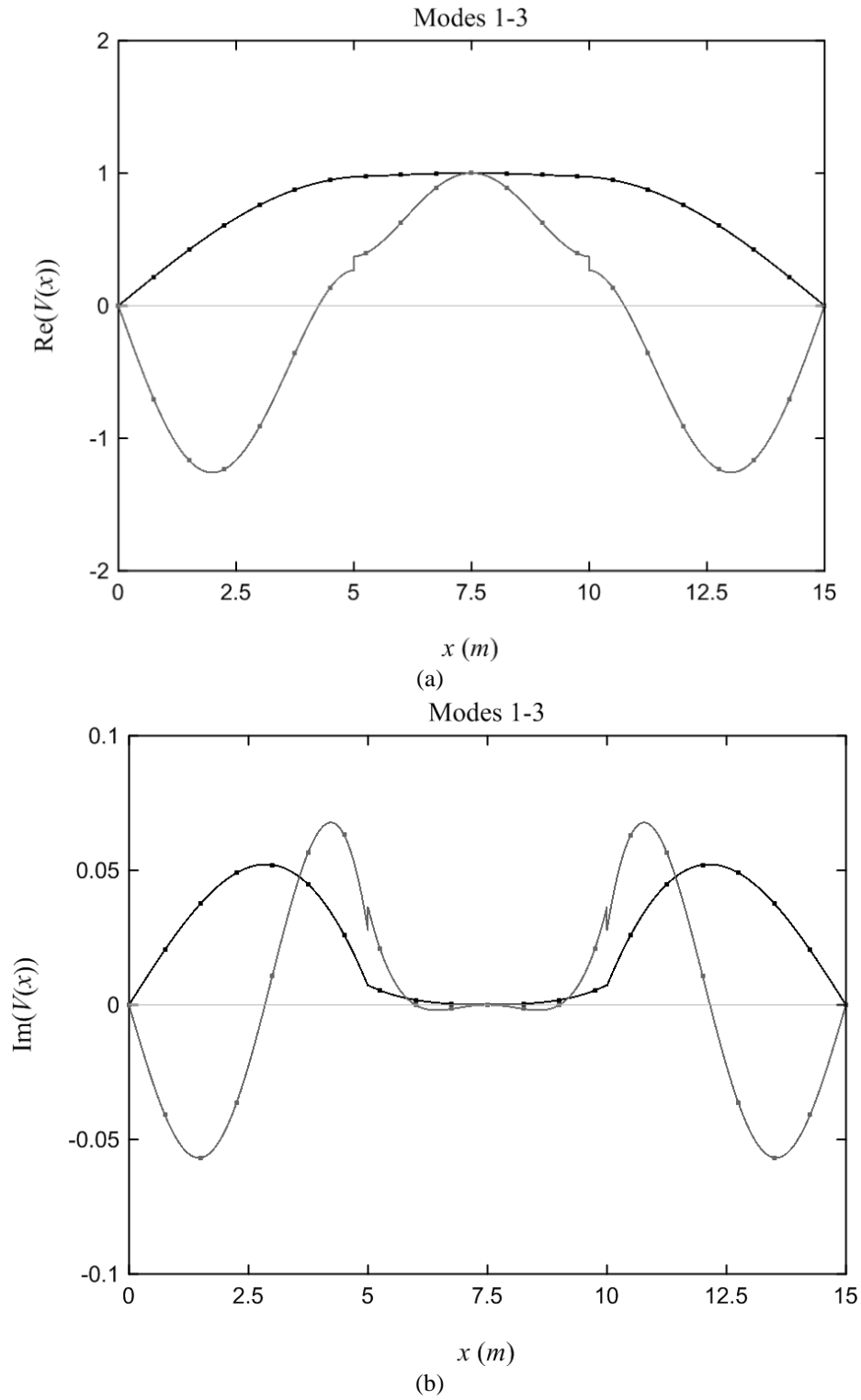


Fig. 3 Deflection eigenfunctions of modes 1-3 of beam in Fig. 2: (a) real part; (b) imaginary part

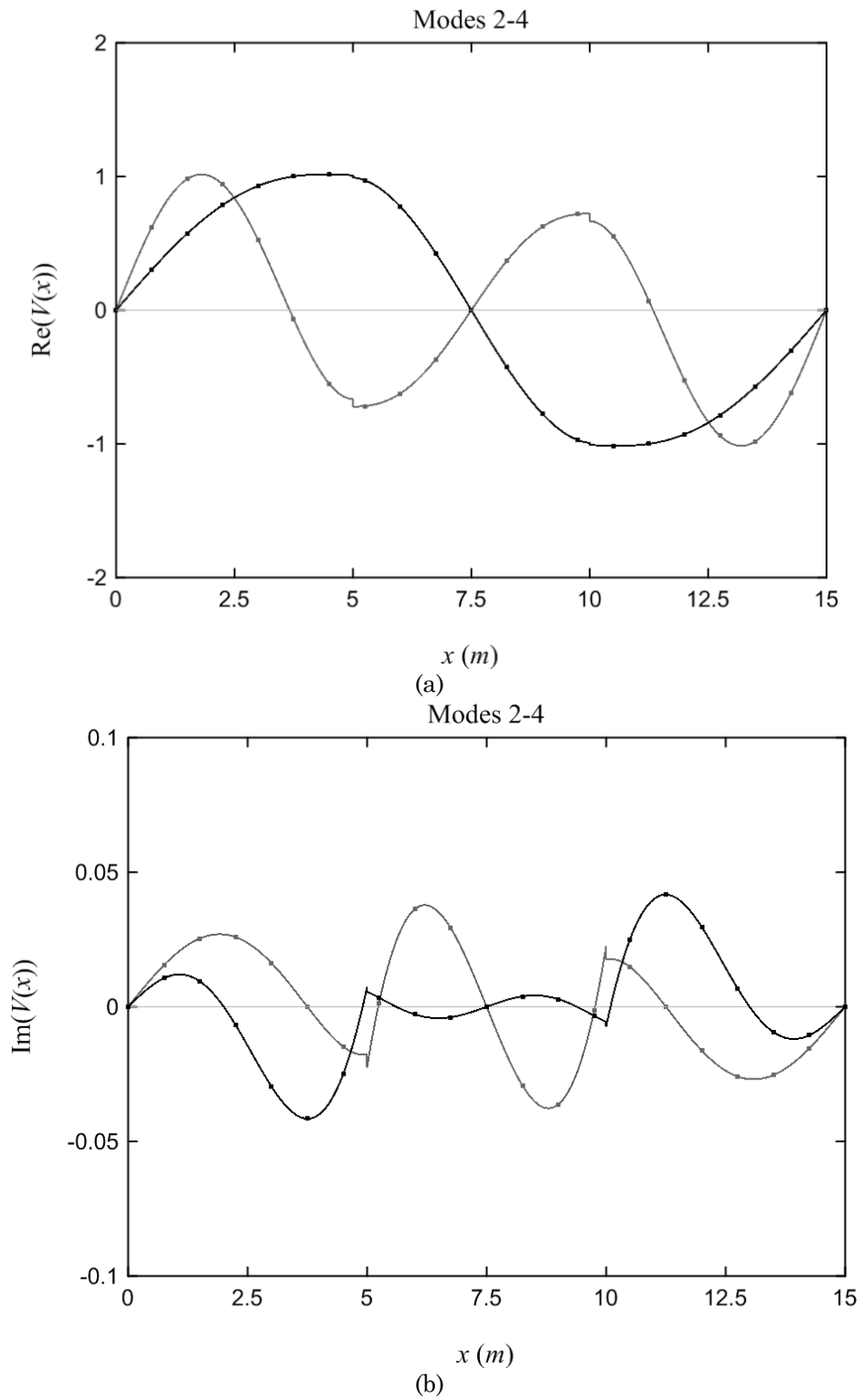


Fig. 4 Deflection eigenfunctions of modes 2-4 of beam in Fig. 2: (a) real part; (b) imaginary part

Table 2 Eigenvalues and damping ratios of first four modes of beam in Fig. 2

	Eigenvalue	Damping ratio
Mode 1	$\pm 46.5273 + 5.1626 i$	0.110282
Mode 2	$\pm 112.217 + 14.428 i$	0.127527
Mode 3	$\pm 306.425 + 13.739 i$	0.044793
Mode 4	$\pm 359.011 + 10.935 i$	0.030444

Table 3 Elements of dynamic stiffness matrix and load vector for beam in Fig. 2.

$\omega = 20 \text{ rad/s}$		
	Eq.(31)	Eq.(B.6)
D_{22}	238856. + 74678.5 i	238856. + 74678.5 i
$D_{23} = D_{32}$	803880. + 131052. i	803880. + 131052. i
$D_{25} = D_{52}$	-128590. - 47128.3 i	-128590. - 47128.3 i
$D_{26} = D_{62}$	377768. + 99700.3 i	377768. + 99700.2 i
D_{33}	$4.23475 \times 10^6 + 363550. i$	$4.23475 \times 10^6 + 363549. i$
$D_{35} = D_{53}$	-377768.0 - 99700.3 i	-377768.0 - 99700.3 i
D_{36}	$1.0995 \times 10^6 + 182826. i$	$1.0995 \times 10^6 + 182826. i$
D_{55}	238856. + 74678.5 i	238856. + 74678.5 i
$D_{56} = D_{65}$	-803880. - 131052. i	-803880. - 131052. i
D_{66}	$4.23475 \times 10^6 + 363550. i$	$4.23475 \times 10^6 + 363550. i$

Fig. 5 shows the DGFs of all response variables for a point load $1 \cdot e^{i\omega t}$ applied at $x_0=L/3$ with forcing frequency $\omega=150 \text{ rad/s}$, as obtained by Eq.(18) (continuous line) and classical method (symbol “*”). Again, real and imaginary parts of the two solutions are in perfect agreement. The proposed solutions inherently satisfy all the required discontinuity conditions at the damper locations. That is, deflection and rotation are discontinuous due to the presence of the internal dampers, while shear force and bending moment are discontinuous due to the external dampers. As in Figs. 3-4, Fig. 5 shows the response variables to the left and right of the damper locations, and Eqs.(38)-(39) can be used to compute deflection and rotation at the application point.

Figs. 6-7 show real and imaginary parts of the deflection DGF for a point load applied at varying position x_0 , as computed by the proposed method. The deflection is symmetric, i.e. $V(x, x_0) = V(x_0, x)$ (Brandt, 2011). Results in Figs. 6-7 coincide with those from the classical method, but comparisons are not shown for brevity.

Fig. 8 shows the deflection DGFs at $x=L/2$ and $x=L/3$, as due to a point load with varying forcing frequency ω and position x_0 . It is well evident that the contribution of the various modes depend on excitation frequency and load position. The contribution of first mode is always dominating. As expected, contributions of second and fourth modes are zero at $x=L/2$, consistently with the shape of the corresponding eigenfunctions, shown in Fig. 4.

Fig. 9 shows the deflection FRFs at $x=L/2$ and $x=L/3$, for uniformly- and linearly-distributed loads over the interval $[L/6, L/2]$, as shown in Fig. 2. Again, the agreement between proposed and

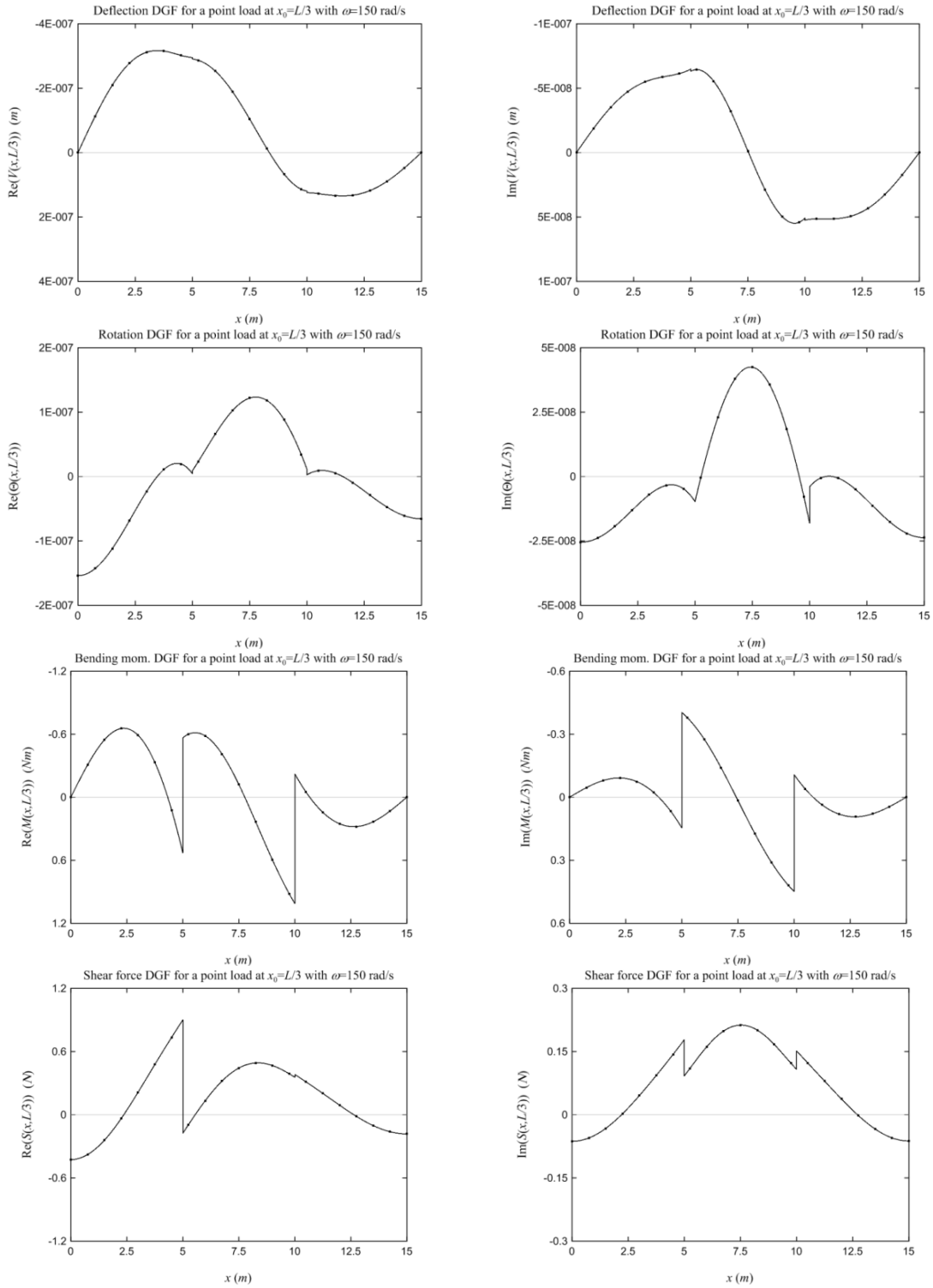


Fig. 5 Dynamic Green's functions of beam in Fig. 2 for a point load with forcing frequency $\omega=150$ rad/s, applied at $x_0=L/3$. Left column: real part; right column: imaginary part.

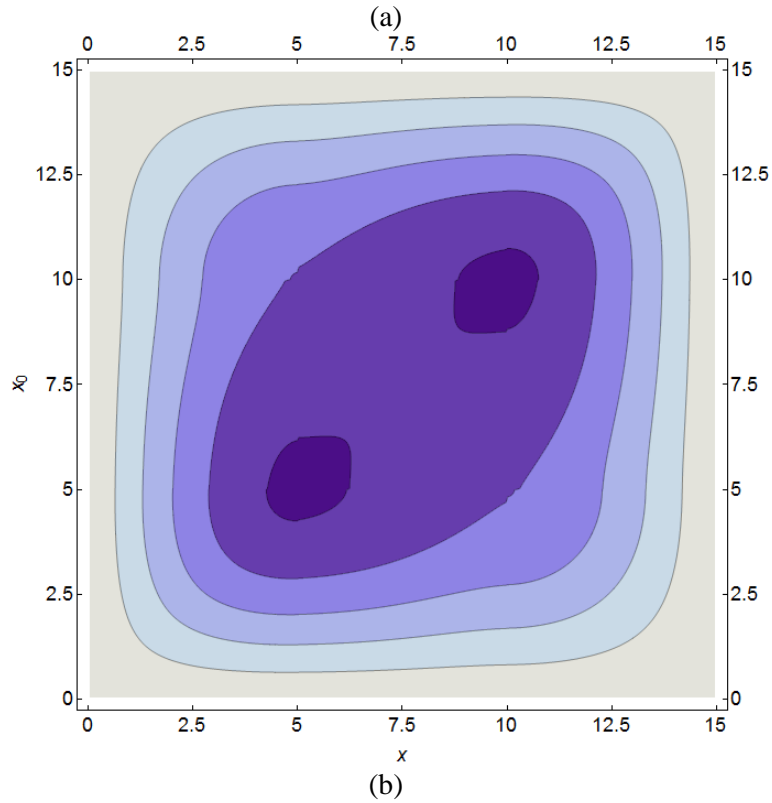
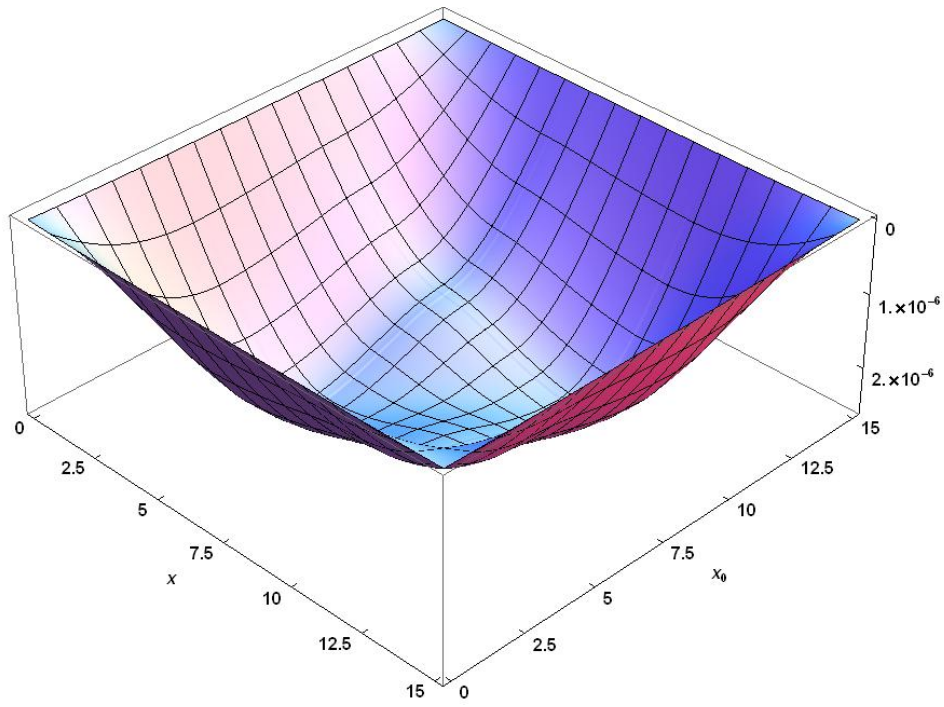
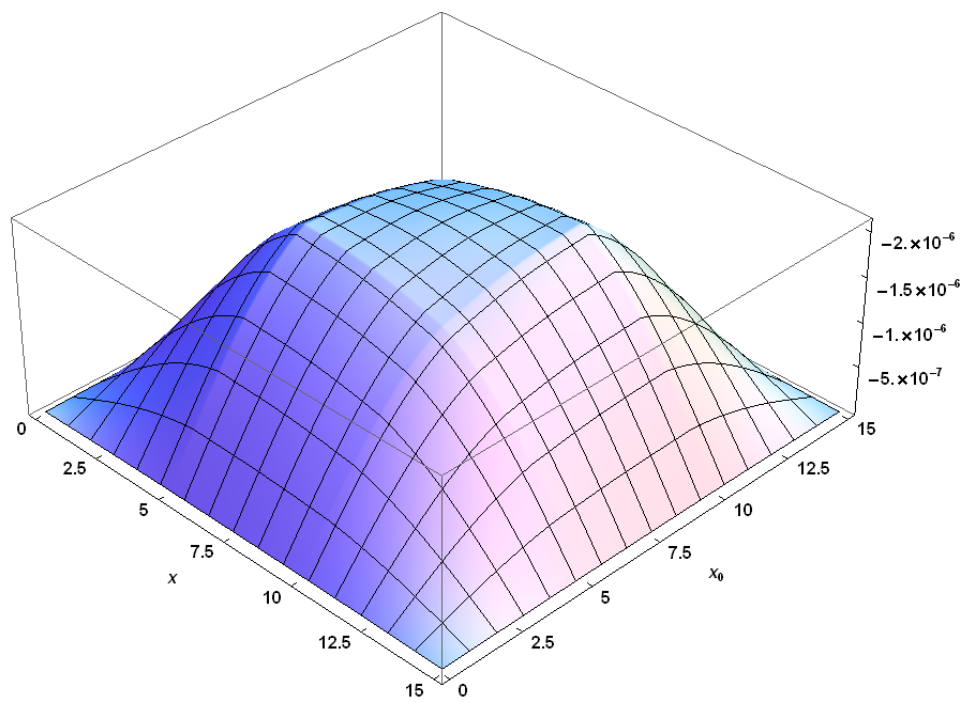
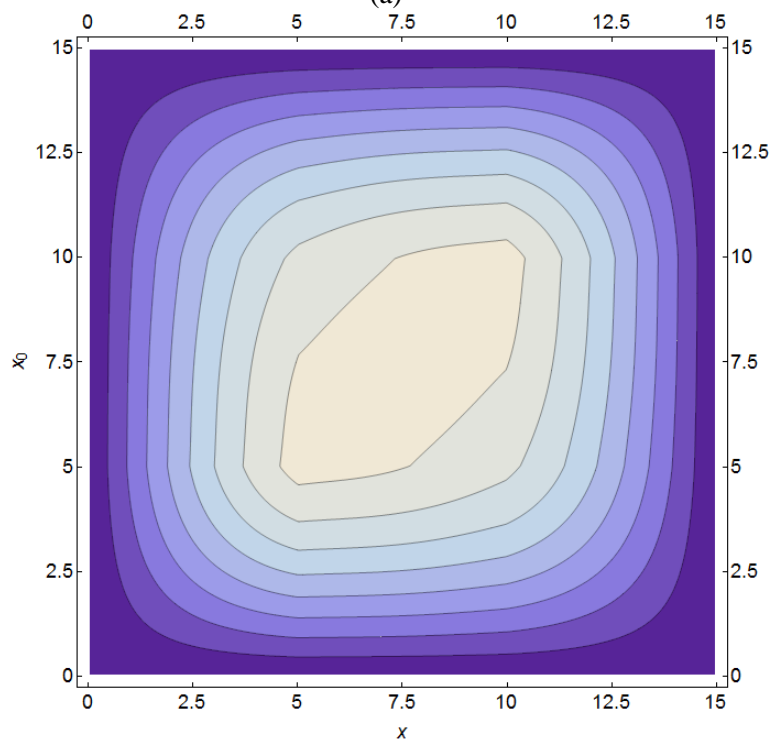


Fig. 6 Deflection dynamic Green's function of beam in Fig. 2 for a point load with forcing frequency $\omega=40$ rad/s, computed at x for various load positions x_0 : (a) real part; (b) contour plot of real part.



(a)



(b)

Fig. 7 Deflection dynamic Green's function of beam in Fig. 2 for a point load with forcing frequency $\omega=40$ rad/s, computed at x for various load positions x_0 : (a) real part; (b) contour plot of real part.

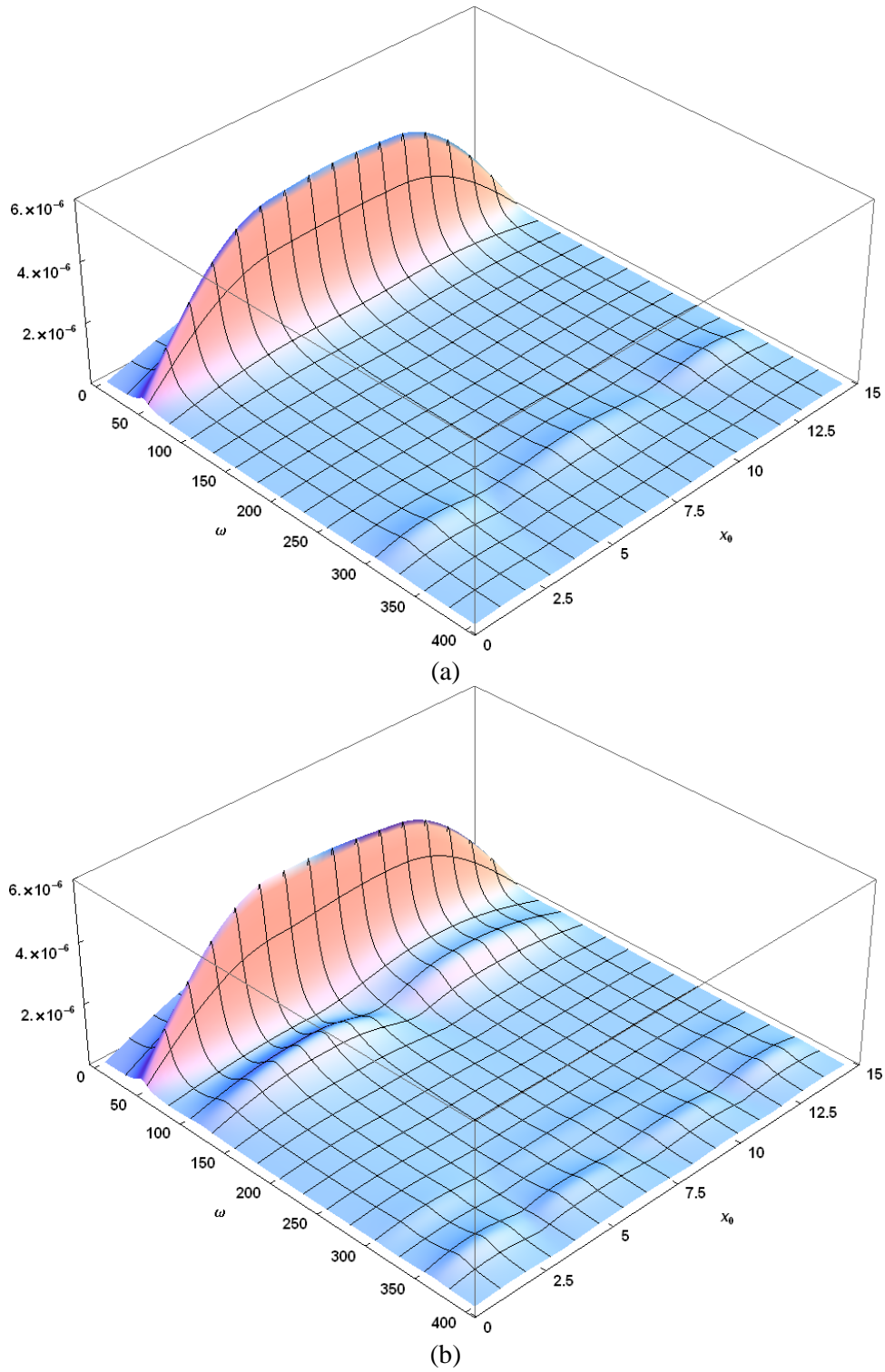


Fig. 8 Deflection dynamic Green's function of beam in Fig. 2 for a point load with varying forcing frequency ω and varying load position x_0 , computed at: (a) $x=L/2$; (b) $x=L/3$.

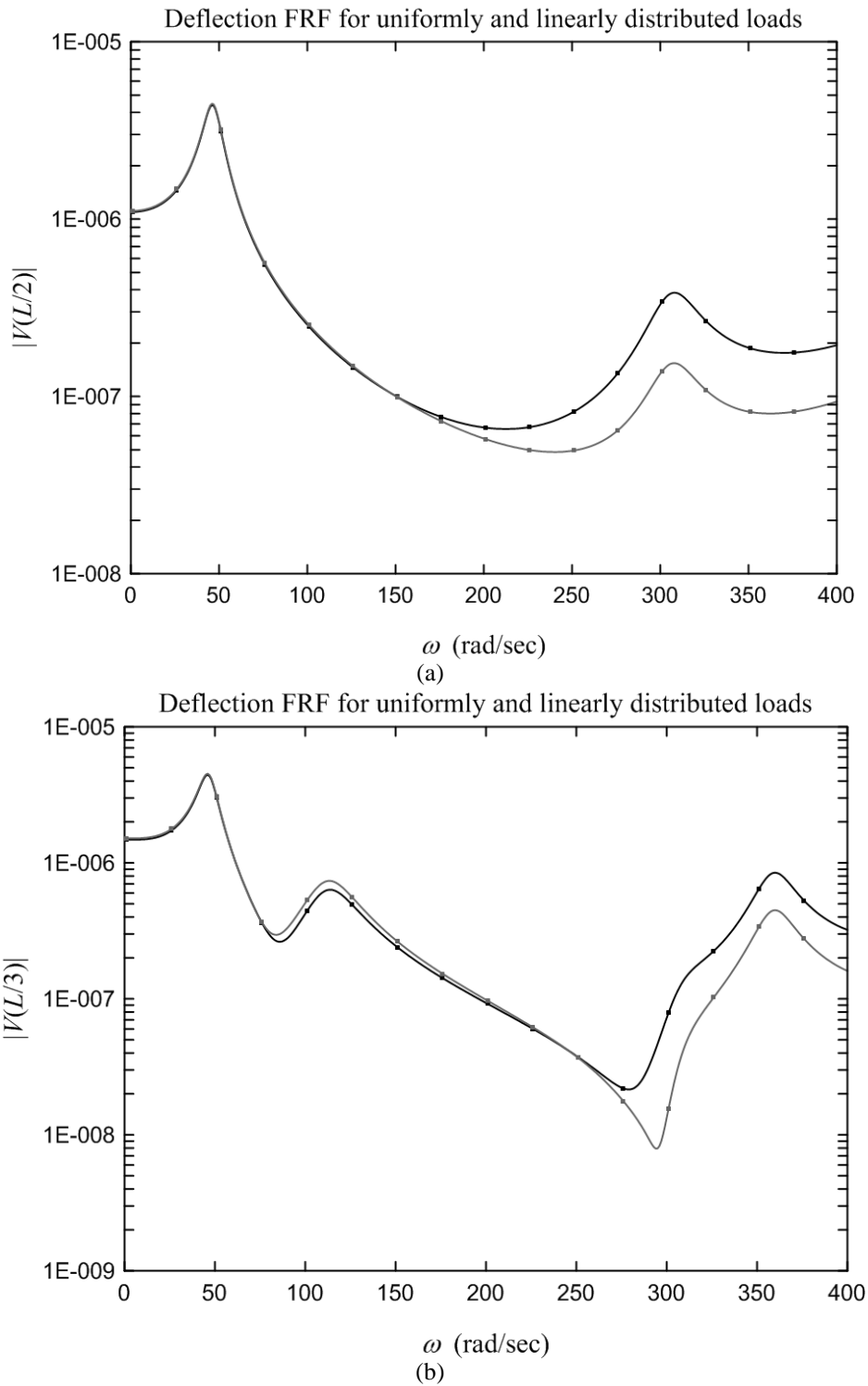


Fig. 9 Deflection frequency response function of beam in Fig. 2 for uniform (black line) and linear (grey line) loads with varying forcing frequency ω , computed at: (a) $x=L/2$; (b) $x=L/3$.

Table 4 Elements of dynamic stiffness matrix and load vector for beam in Fig. 2.

$\omega = 20 \text{ rad/s} - \text{uniform load}$		
	Eq.(36)	Eq.(B.7)
$f_2^{(0)}$	$-0.583334 + 0.00930356 i$	$-0.583334 + 0.00930356 i$
$f_3^{(0)}$	$-1.47582 + 0.125022 i$	$-1.47582 + 0.125022 i$
$f_5^{(0)}$	$-0.210926 - 0.0192521 i$	$-0.210926 - 0.0192521 i$
$f_6^{(0)}$	$0.604232 - 0.00133359 i$	$0.604232 - 0.00133359 i$

Table 5 Elements of dynamic stiffness matrix and load vector for beam in Fig. 2.

$\omega = 20 \text{ rad/s} - \text{linear load}$		
	Eq.(36)	Eq.(B.7)
$f_2^{(0)}$	$-0.576563 + 0.00970668 i$	$-0.576563 + 0.00970668 i$
$f_3^{(0)}$	$-1.53058 + 0.141108 i$	$-1.53058 + 0.141108 i$
$f_5^{(0)}$	$-0.204916 - 0.0213591 i$	$-0.204916 - 0.0213591 i$
$f_6^{(0)}$	$0.587722 + 0.00623944 i$	$0.587722 + 0.00623944 i$

classical solutions is excellent.

Finally, the elements of the dynamic stiffness $\mathbf{D}(\omega)$ matrix and load vector \mathbf{f}_0 are reported in Tables 3-4-5 for different frequencies ω , as computed by Eqs.(31)-(36) and Eqs.(B.6)-(B.7) in Appendix B. Again, the two solutions coincide.

5. Conclusions

This paper has addressed the frequency response of beams under harmonically-varying point/polynomial loads, which carry multiple external/internal Kelvin-Voigt viscoelastic dampers at the same position, modeling external damping devices and internal damping due to damage or imperfect connections. A solution recently proposed by the author (Failla 2016b) has been revisited, presenting an original formulation of exact dynamic stiffness matrix and load vector, with advantages with a previous one (Failla 2016b).

The proposed solutions are exact and fulfill the required conditions at the locations of dampers/point loads. They can readily be implemented for any number and positions of dampers, positions of point/polynomial loads, with significant advantages over the exact classical approach and the standard FE method, as discussed throughout the paper. The proposed solutions appear particularly suitable for investigating frequency response as damper/load positions change, as is typical in identification or optimization problems.

Finally, it is worth noticing that the frequency analysis approach of this paper is not restricted to Kelvin-Voigt viscoelastic dampers, but applies for any damper with constitutive law for which a Fourier transform is available in a closed form (examples may be found in recent papers by Ding *et al.* (2016), Li and Hu (2016)). This is a relevant advantage in recognition of the fact that, in some cases, Kelvin-Voigt viscoelasticity does not prove adequate to fit experimental behavior of

dampers. From the frequency-domain solutions built as explained in this paper, impulse response functions can readily be obtained by a standard inverse Fourier transform (Clough and Penzien 2003), in order to build the time-domain numerical response of the beam with multiple dampers.

Further effort will be devoted to formulate the proposed approach for TM beams with multiple dampers. For this purpose, pertinent closed-form solutions of the TM beam motion equation shall be built, under discontinuity-related generalized functions as in Eqs.(2)-(3) of this paper.

References

- Abdel Raheem, S.E. (2014), “Analytical and numerical algorithm for exploring dynamic response of non-classically damped hybrid structures”, *Coupled Syst. Mech.*, **3**(2), 171-193.
- Abu-Hilal, M. (2003), “Forced vibration of Euler-Bernoulli beams by means of dynamic Green functions”, *J. Sound Vib.*, **267**(2), 191-207.
- Alsaif, K. and Foda, M.A. (2002), “Vibration suppression of a beam structure by intermediate masses and springs”, *J. Sound Vib.*, **256**(4), 629-645.
- Bambill, D.V. and Rossit, C.A. (2002), “Forced vibrations of a beam elastically restrained against rotation and carrying a spring-mass system”, *Ocean Eng.*, **29**(6), 605-626.
- Brandt, A. (2011), *Noise and Vibration Analysis: Signal Analysis and Experimental Procedures*, John Wiley and Sons, Chichester, U.K.
- Caddemi, S., Caliò, I. and Cannizzaro, F. (2013a), “Closed-form solutions for stepped Timoshenko beams with internal singularities and along-axis external supports”, *Arch. Appl. Mech.*, **83**(4), 559-577.
- Caddemi, S., Caliò, I. and Cannizzaro, F. (2013b), “The influence of multiple cracks on tensile and compressive buckling of shear deformable beams”, *Int. J. Solids Struct.*, **50**(20-21), 3166-3183.
- Caddemi, S., Caliò, I. and Cannizzaro, F. (2015), “Influence of an elastic end support on the dynamic stability of Beck’s column with multiple weak sections”, *Int. J. Non-Linear Mech.*, **69**, 14-28.
- Clough, R.W. and Penzien, J. (2003), *Dynamics of Structures*, Computers & Structures Inc., Berkeley, CA, USA.
- Ding, Z., Li, L., Hu, Y., Li, X. and Deng, W. (2016), “State-space based time integration method for structural systems involving multiple nonviscous damping models”, *Comput. Struct.*, **171**, 31-45.
- Failla, G. (2014), “On the dynamics of viscoelastic discontinuous beams”, *Mech. Res. Commun.*, **60**, 52-63.
- Failla, G. (2016a), “An exact generalised function approach to frequency response analysis of beams and plane frames with the inclusion of viscoelastic damping”, *J. Sound Vib.*, **360**, 171-202.
- Failla, G. (2016b), “Stationary response of beams and frames with fractional dampers via exact frequency response functions”, *J. Eng. Mech.*, doi: 10.1061/(ASCE)EM.1943-7889.0001076.
- Failla, G. and Santini, A. (2007), “On Euler-Bernoulli discontinuous beam solutions via uniform-beam Green’s functions”, *Int. J. Solids Struct.*, **44**(22), 7666-7687.
- Falsone, G. (2002), “The use of generalised functions in the discontinuous beam bending differential equation”, *Int. J. Eng. Educ.*, **18**(3), 337-343.
- Foda, M.A. and Albassam, B.A. (2006), “Vibration confinement in a general beam structure during harmonic excitations”, *J. Sound Vib.*, **295**(3), 491-517.
- Guo, Y.Q. and Chen, W.Q. (2007), “Dynamic analysis of space structures with multiple tuned mass dampers”, *Eng. Struct.*, **29**(12), 3390-3403.
- Gürgöze, M. and Erol, H. (2002), “On the frequency response function of a damped cantilever simply supported in-span and carrying a tip mass”, *J. Sound Vib.*, **255**(3), 489-500.
- Hanss, M., Oexl, S. and Gaul, L. (2002), “Identification of a bolted-joint model with fuzzy parameters loaded normal to the contact interface”, *Mech. Res. Commun.*, **29**(2-3), 177-187.
- Hong, S.W. and Kim, J.W. (1999), “Modal analysis of multi-span Timoshenko beams connected or supported by resilient joints with damping”, *J. Sound Vib.*, **227**(4), 787-806.
- Housner, G.W., Bergman, L.A., Caughey, T.K., Chassiakos, A.G., Claus, R.O., Masri, S.F. *et al.* (1997),

- “Structural control: Past, present, and future”, *ASCE J. Eng. Mech.*, **123**(9), 897-971.
- Kareem, A. and Kline, S. (1995), “Performance of multiple mass dampers under random loading”, *J. Struct. Eng.*, **121**(2), 348-361.
- Kawashima, S. and Fujimoto, T. (1984), “Vibration analysis of frames with semi-rigid connections”, *Comput. Struct.*, **19**(1), 85-92.
- Keivani, A., Shooshtari, A. and Aftabi Sani, A. (2014), “Forced vibration analysis of a dam-reservoir interaction problem in frequency domain”, *Coupled Syst. Mech.*, **3**(4), 385-403.
- Khiem, N.T. and Lien, T.V. (2002), “The dynamic stiffness matrix method in forced vibration analysis of multiple-cracked beam”, *J. Sound Vib.*, **254**(3), 541-555.
- Lewandowski, R. and Grzymisławska, J. (2009), “Dynamic analysis of structures with multiple tuned mass dampers”, *J. Civ. Eng. Manag.*, **15**(1), 77-86.
- Li, L., Hu, Y. and Wang, X. (2014), “Eliminating the modal truncation problem encountered in frequency responses of viscoelastic systems”, *J. Sound Vib.*, **333**(4), 1182-1192.
- Li, L., Hu, Y., Wang, X. and Lü, L. (2014), “A hybrid expansion method for frequency response functions of non-proportionally damped systems”, *Mech. Syst. Signal Process.*, **42**(1), 31-41.
- Li, L. and Hu, Y. (2016), “State-space method for viscoelastic systems involving general damping model”, *AIAA Journal*, DOI: 10.2514/1.J054180.
- Lin, H.Y. (2008), “Dynamic analysis of a multi-span uniform beam carrying a number of various concentrated elements”, *J. Sound Vib.*, **309**(1), 262-275.
- Maximov, J.T. (2014), “A new approach to modeling the dynamic response of Bernoulli-Euler beam under moving load”, *Coupled Syst. Mech.*, **3**(3), 247-265.
- Oliveto, G., Santini, A. and Tripodi, E. (1997), “Complex modal analysis of a flexural vibrating beam with viscous end conditions”, *J. Sound Vib.* **200**(3), 327-345.
- Ou, J.P., Long, X. and Li, Q.S. (2007), “Seismic response analysis of structures with velocity-dependent dampers”, *J. Constr. Steel Res.*, **63**(5), 628-638.
- Sadek, F., Mohraz, B., Taylor, A.W. and Chung, R.M. (1997), “A method of estimating the parameters of tuned mass dampers for seismic applications”, *Earthq. Eng. Struct. Dyn.*, **26**(6), 617-635.
- Sarvestan, V., Mirdamadi, H.R., Ghayour, M. and Mokhtari, A. (2015), “Spectral finite element for vibration analysis of cracked viscoelastic Euler-Bernoulli beam subjected to moving load”, *Acta Mech.*, **226**(12), 4259-4280.
- Sekulovic, M., Salatic, R. and Nefovska M. (2002), “Dynamic analysis of steel frames with flexible connections”, *Comput. Struct.*, **80**(11), 935-955.
- Shafiei, M. and Khaji, N. (2011), “Analytical solutions for free and forced vibrations of a multiple cracked Timoshenko beam subject to a concentrated moving load”, *Acta Mech.*, **221**(1-2), 79-97.
- Soong, T.T. and Spencer, B.F. (2002), “Supplemental energy dissipation: state-of-the-art and state-of-the-practice”, *Eng. Struct.*, **24**(3), 243-259.
- Sorrentino, S., Fasana, A. and Marchesiello, S. (2004), “Frequency domain analysis of continuous systems with viscous generalized damping”, *Shock Vib.*, **11**(3-4), 243-259.
- Sorrentino, S., Marchesiello, S. and Piombo, B.A.D. (2003), “A new analytical technique for vibration analysis of non-proportionally damped beams”, *J. Sound Vib.*, **265**(4), 765-782.
- Sorrentino, S., Fasana, A. and Marchesiello, S. (2007), “Analysis of non-homogeneous Timoshenko beams with generalized damping distributions”, *J. Sound Vib.*, **304**(3), 779-792.
- Wang, J. and Qiao, P. (2007), “Vibration of beams with arbitrary discontinuities and boundary conditions”, *J. Sound Vib.*, **308**(1), 12-27.
- Wolfram Research Inc. (2008), *Mathematica Version 7.0*, Champaign, IL, USA.
- Wu, J.S. and Chen, D.W. (2000), “Dynamic analysis of a uniform cantilever beam carrying a number of elastically mounted point masses with dampers”, *J. Sound Vib.*, **229**(3), 549-578.
- Xu, Y.L. and Zhang, W.S. (2001), “Modal analysis and seismic response of steel frames with connection dampers”, *Eng. Struct.*, **23**(4), 385-396.
- Xu, H. and Li, W.L. (2008), “Dynamic behavior of multi-span bridges under moving loads with focusing on the effect of the coupling conditions between spans”, *J. Sound Vib.*, **312**(4), 736-753.

Yavari, A., Sarkani, S. and Moyer, E.T. (2000), "On applications of generalized functions to beam bending problems", *Int. J. Solids Struct.*, **37**(40), 5675-5705.

Appendix A

To derive terms of matrix $\mathbf{\Omega}(x)$ in Eq.(14) and vectors $\mathbf{J}^{(r)}(x, x_j)$ in Eqs.(16) for $r=P, W, \Delta V$ and $\Delta\Theta$, first consider the following steady-state motion equations of the beam under harmonic unit point load, unit moment, relative displacement, given as

(A.1)

$$EI \frac{\bar{d}^4 V(x)}{dx^4} - m_0 \omega^2 V(x) - \sum_{j=1}^n P \cdot \delta(x - x_j) + \sum_{j=1}^n W \cdot \delta^{(1)}(x - x_j) - \sum_{j=1}^n EI \cdot \Delta\Theta \cdot \delta^{(2)}(x - x_j) - \sum_{j=1}^n EI \cdot \Delta V \cdot \delta^{(3)}(x - x_j) = 0$$

(A.2)

with $P=1, W=1, \Delta V=1$ and $\Delta\Theta=1$. Using integration by parts, the following relations can be derived among the particular solution $J_V^{(P)}(x, x_0)$ due to a unit point load $P=1$, the particular solution $J_V^{(W)}(x, x_0)$ due to a unit moment $W=1$, the particular solution $J_V^{(\Delta V)}(x, x_0)$ due to a unit relative deflection $\Delta V=1$, and the particular solution $J_V^{(\Delta\Theta)}(x, x_0)$ due to a unit relative rotation $\Delta\Theta=1$:

$$J_V^{(W)}(x, x_0) = - \int_0^L J_V^{(P)}(x, \xi) \delta^{(1)}(\xi - x_0) d\xi = \frac{\bar{d} J_V^{(P)}(x, x_0)}{dx_0}$$

(A.3)

$$J_V^{(\Delta\Theta)}(x, x_0) = EI \int_0^L J_V^{(P)}(x, \xi) \delta^{(2)}(\xi - x_0) d\xi = EI \frac{\bar{d}^2 J_V^{(P)}(x, x_0)}{dx_0^2}$$

(A.4)

$$J_V^{(\Delta V)}(x, x_0) = EI \int_0^L J_V^{(P)}(x, \xi) \delta^{(3)}(\xi - x_0) d\xi = -EI \frac{\bar{d}^3 J_V^{(P)}(x, x_0)}{dx_0^3}$$

(A.5)

Next, starting from the solution of the homogeneous equation associated with Eq.(A.2) and the particular integral $J_V^{(P)}(x, x_0)$ due to a unit point load $P=1$, which are readily available in a closed form by Mathematica (Wolfram 2008), and using Eqs.(A.1), (A.3)-(A.5), terms in matrix $\mathbf{\Omega}(x)$ and vectors $\mathbf{J}^{(r)}(x, x_j)$ for $r = P, W, \Delta U, \Delta\Theta$ are obtained as (obviously, terms in matrix $\mathbf{\Omega}(x)$ do not depend on the loading function and, for this, do not carry superscript (r):

$$\begin{aligned}
\Omega_{v_1}(x) &= e^{-\beta x}; & \Omega_{v_2}(x) &= e^{\beta x}; & \Omega_{v_3}(x) &= \cos(\beta x); & \Omega_{v_4}(x) &= \sin(\beta x) \\
\Omega_{\theta_1}(x) &= -\beta e^{-\beta x}; & \Omega_{\theta_2}(x) &= \beta e^{\beta x}; & \Omega_{\theta_3}(x) &= -\beta \sin(\beta x); & \Omega_{\theta_4}(x) &= \beta \cos(\beta x) \\
\Omega_{M_1}(x) &= -EI\beta^2 e^{-\beta x}; & \Omega_{M_2}(x) &= -EI\beta^2 e^{\beta x}; & \Omega_{M_3}(x) &= EI\beta^2 \cos(\beta x); & \Omega_{M_4}(x) &= EI\beta^2 \sin(\beta x) \\
\Omega_{S_1}(x) &= EI\beta^3 e^{-\beta x}; & \Omega_{S_2}(x) &= -EI\beta^3 e^{\beta x}; & \Omega_{S_3}(x) &= -EI\beta^3 \sin(\beta x); & \Omega_{S_4}(x) &= EI\beta^3 \cos(\beta x)
\end{aligned} \tag{A.6a-p}$$

Particular integrals $\mathbf{J}^{(P)}(x, x_0)$ for a point load $P = 1$ at $x = x_0$

$$J_V^{(P)}(x, x_0) = \alpha [\sinh(\beta(x - x_0)) - \sin(\beta(x - x_0))] H(x - x_0) \tag{A.7}$$

$$J_\Theta^{(P)}(x, x_0) = \frac{\bar{d} J_V^{(P)}(x, x_0)}{dx} = \alpha \beta [\cosh(\beta(x - x_0)) - \cos(\beta(x - x_0))] H(x - x_0) \tag{A.8}$$

$$J_M^{(P)}(x, x_0) = -EI \frac{\bar{d}^2 J_V^{(P)}(x, x_0)}{dx^2} = -EI \alpha \beta^2 [\sinh(\beta(x - x_0)) + \sin(\beta(x - x_0))] H(x - x_0) \tag{A.9}$$

$$J_S^{(P)}(x, x_0) = -EI \frac{\bar{d}^3 J_V^{(P)}(x, x_0)}{dx^3} = -EI \alpha \beta^3 [\cosh(\beta(x - x_0)) + \cos(\beta(x - x_0))] H(x - x_0) \tag{A.10}$$

Particular integrals $\mathbf{J}^{(W)}(x, x_0)$ for a point moment $W = 1$ at $x = x_0$

$$J_V^{(W)}(x, x_0) = \frac{\bar{d} J_V^{(P)}(x, x_0)}{dx_0} = -\alpha \beta [\cosh(\beta(x - x_0)) - \cos(\beta(x - x_0))] H(x - x_0) \tag{A.11}$$

$$J_\Theta^{(W)}(x, x_0) = \frac{\bar{d} J_V^{(W)}(x, x_0)}{dx} = -\alpha \beta^2 [\sinh(\beta(x - x_0)) + \sin(\beta(x - x_0))] H(x - x_0) \tag{A.12}$$

$$J_M^{(W)}(x, x_0) = -EI \frac{\bar{d}^2 J_V^{(W)}(x, x_0)}{dx^2} = EI \alpha \beta^3 [\cosh(\beta(x - x_0)) + \cos(\beta(x - x_0))] H(x - x_0) \tag{A.13}$$

$$J_S^{(W)}(x, x_0) = -EI \frac{\bar{d}^3 J_V^{(W)}(x, x_0)}{dx^3} - 1 \cdot \delta(x - x_0) = EI \alpha \beta^4 [\sinh(\beta(x - x_0)) - \sin(\beta(x - x_0))] H(x - x_0) \tag{A.14}$$

Particular integrals $\mathbf{J}^{(\Delta\Theta)}(x, x_0)$ for a relative rotation $\Delta\Theta=1$ at $x=x_0$

$$J_V^{(\Delta\Theta)}(x, x_0) = EI \frac{\bar{d}^2 J_V^{(P)}(x, x_0)}{dx_0^2} = EI \alpha \beta^2 \left[\sinh(\beta(x-x_0)) + \sin(\beta(x-x_0)) \right] H(x-x_0) \quad (\text{A.15})$$

$$J_\Theta^{(\Delta\Theta)}(x, x_0) = \frac{\bar{d} J_V^{(\Delta\Theta)}(x, x_0)}{dx} = EI \alpha \beta^3 \left[\cosh(\beta(x-x_0)) + \cos(\beta(x-x_0)) \right] H(x-x_0) \quad (\text{A.16})$$

$$J_M^{(\Delta\Theta)}(x, x_0) = -EI \frac{\bar{d}^2 J_V^{(\Delta\Theta)}(x, x_0)}{dx^2} + EI \cdot \delta(x-x_0) = -EI^2 \alpha \beta^4 \left[\sinh(\beta(x-x_0)) - \sin(\beta(x-x_0)) \right] H(x-x_0) \quad (\text{A.17})$$

$$J_S^{(\Delta\Theta)}(x, x_0) = -EI \frac{\bar{d}^3 J_V^{(\Delta\Theta)}(x, x_0)}{dx^3} + EI \cdot \delta^{(1)}(x-x_0) = -EI^2 \alpha \beta^5 \left[\cosh(\beta(x-x_0)) - \cos(\beta(x-x_0)) \right] H(x-x_0) \quad (\text{A.18})$$

Particular integrals $\mathbf{J}^{(\Delta V)}(x, x_0)$ for a relative deflection $\Delta V=1$ at $x=x_0$

$$J_V^{(\Delta V)}(x, x_0) = -EI \frac{\bar{d}^3 J_V^{(P)}(x, x_0)}{dx_0^3} = EI \alpha \beta^3 \left[\cosh(\beta(x-x_0)) + \cos(\beta(x-x_0)) \right] H(x-x_0) \quad (\text{A.19})$$

$$J_\Theta^{(\Delta V)}(x, x_0) = \frac{\bar{d} J_V^{(\Delta V)}(x, x_0)}{dx} - 1 \cdot \delta(x-x_0) = EI \alpha \beta^4 \left[\sinh(\beta(x-x_0)) - \sin(\beta(x-x_0)) \right] H(x-x_0) \quad (\text{A.20})$$

$$J_M^{(\Delta V)}(x, x_0) = -EI \frac{\bar{d}^2 J_V^{(\Delta V)}(x, x_0)}{dx^2} + EI \cdot \delta^{(1)}(x-x_0) = -EI^2 \alpha \beta^5 \left[\cosh(\beta(x-x_0)) - \cos(\beta(x-x_0)) \right] H(x-x_0) \quad (\text{A.21})$$

$$J_S^{(\Delta V)}(x, x_0) = -EI \frac{\bar{d}^3 J_V^{(\Delta V)}(x, x_0)}{dx^3} + EI \cdot \delta^{(2)}(x-x_0) = -EI^2 \alpha \beta^6 \left[\sinh(\beta(x-x_0)) + \sin(\beta(x-x_0)) \right] H(x-x_0) \quad (\text{A.22})$$

In Eqs.(A.6)-(A.22), $\alpha = \alpha(\omega) = 2^{-1} EI^{-1/4} m_0^{-3/4} \omega^{-3/2}$, $\beta = \beta(\omega) = EI^{-1/4} m_0^{1/4} \omega^{1/2}$, and $EI \alpha \beta^3 = 1/2$.

Interestingly, notice that the particular integrals are all continuous through the whole domain, except for $x=x_0$ where appropriate, i.e.:

$$\begin{aligned}
J_S^{(P)}(x_0^+, x_0) - J_S^{(P)}(x_0^-, x_0) &= -1 \\
J_M^{(W)}(x_0^+, x_0) - J_M^{(W)}(x_0^-, x_0) &= 1 \\
J_\Theta^{(\Delta\Theta)}(x_0^+, x_0) - J_\Theta^{(\Delta\Theta)}(x_0^-, x_0) &= 1 \\
J_V^{(\Delta V)}(x_0^+, x_0) - J_V^{(\Delta V)}(x_0^-, x_0) &= 1
\end{aligned} \tag{A.23}$$

Next, consider Eq.(17) for $\mathbf{Y}^{(f)}(x)$, which represents the particular solutions related to the applied load. In view of the analytical expressions of $\mathbf{J}^{(P)}(x, \xi)$ given in this Appendix, it can be seen that every integral in Eq.(17) can be reverted to the general form $\int_a^b g(\xi)H(x-\xi)d\xi$, with $g(\xi)$ given by the product of the loading function and certain trigonometric/hyperbolic functions. For instance, in view of Eq.(A.7) for $J_V^{(P)}(x, x_0)$, computing $\mathbf{Y}^{(f)}(x)$ will involve, among others, the integral

$$\int_a^b J_V^{(P)}(x, \xi) f(\xi) d\xi = \int_a^b g(\xi) H(x-\xi) d\xi, \quad g(\xi) = f(\xi) \alpha [\sinh(\beta(x-\xi)) - \sin(\beta(x-\xi))] \tag{A.24}$$

Using the theory of generalized functions, integrals $\int_a^b g(\xi)H(x-\xi)d\xi$ can be computed as:

$$\begin{aligned}
\int_a^b g(\xi)H(x-\xi)d\xi &= \left\{ H(x-\xi) \left[g^{[1]}(\xi) - g^{[1]}(x) \right] \right\}_a^b = \\
&= H(x-b) \left[g^{[1]}(b) - g^{[1]}(x) \right] - H(x-a) \left[g^{[1]}(a) - g^{[1]}(x) \right]
\end{aligned} \tag{A.25}$$

where $g^{[1]}$ denotes the first-order primitive function of $g(\xi)$. It is noticed that, for polynomial loads $f(x)$ typically encountered in engineering applications, the first-order primitive $g^{[1]}$ can be obtained in a closed form by any symbolic package as, for instance, Mathematica (Wolfram 2008). This means that, upon deriving closed-form expressions of \mathbf{c} from Eq.(24), Eq.(18) provides the exact closed-form expressions of the FRFs beam with an arbitrary number of dampers, due to polynomial loads $f(x)e^{i\omega t}$, for all response variables.

Appendix B

The exact dynamic stiffness matrix (31) and load vector (36) can be derived by an alternative procedure (Failla 2016), here recalled for convenience.

Eq.(18) and Eqs.(33)-(34) for the frequency response can be used to build the nodal equations

$$\mathbf{u} = \mathbf{\Gamma} \mathbf{b} + \mathbf{u}^{(f)} \quad (\text{B.1})$$

$$\mathbf{f} = \mathbf{\Xi} \mathbf{b} + \mathbf{f}^{(f)} \quad (\text{B.2})$$

$$\text{for } \mathbf{u}^{(f)} = \begin{bmatrix} 0 & \tilde{v}^{(f)}(0) & \tilde{\theta}^{(f)}(0) & 0 & \tilde{v}^{(f)}(L) & \tilde{\theta}^{(f)}(L) \end{bmatrix}^T$$

$$\mathbf{f}^{(f)} = \begin{bmatrix} 0 & -\tilde{s}^{(f)}(0) & \tilde{M}^{(f)}(0) & 0 & \tilde{s}^{(f)}(L) & -\tilde{M}^{(f)}(L) \end{bmatrix}^T, \mathbf{b} = [a_1 \quad a_2 \quad c_1 \quad c_2 \quad c_3 \quad c_4]^T, \text{ while } \mathbf{\Gamma} \text{ and } \mathbf{\Xi} \text{ are}$$

$$\mathbf{\Gamma} = \begin{bmatrix} U_{11}(0) & U_{12}(0) & 0 & 0 & 0 & 0 \\ 0 & 0 & (\tilde{\mathbf{Y}}(0))_{1,1} & (\tilde{\mathbf{Y}}(0))_{1,2} & (\tilde{\mathbf{Y}}(0))_{1,3} & (\tilde{\mathbf{Y}}(0))_{1,4} \\ 0 & 0 & (\tilde{\mathbf{Y}}(0))_{2,1} & (\tilde{\mathbf{Y}}(0))_{2,2} & (\tilde{\mathbf{Y}}(0))_{2,3} & (\tilde{\mathbf{Y}}(0))_{2,4} \\ U_{11}(L) & U_{12}(L) & 0 & 0 & 0 & 0 \\ 0 & 0 & (\tilde{\mathbf{Y}}(L))_{1,1} & (\tilde{\mathbf{Y}}(L))_{1,2} & (\tilde{\mathbf{Y}}(L))_{1,3} & (\tilde{\mathbf{Y}}(L))_{1,4} \\ 0 & 0 & (\tilde{\mathbf{Y}}(L))_{2,1} & (\tilde{\mathbf{Y}}(L))_{2,2} & (\tilde{\mathbf{Y}}(L))_{2,3} & (\tilde{\mathbf{Y}}(L))_{2,4} \end{bmatrix} \quad (\text{B.3})$$

$$\mathbf{\Xi} = \begin{bmatrix} -N_{11}(0) & -N_{12}(0) & 0 & 0 & 0 & 0 \\ 0 & 0 & -(\tilde{\mathbf{Y}}(0))_{4,1} & -(\tilde{\mathbf{Y}}(0))_{4,2} & -(\tilde{\mathbf{Y}}(0))_{4,3} & -(\tilde{\mathbf{Y}}(0))_{4,4} \\ 0 & 0 & (\tilde{\mathbf{Y}}(0))_{3,1} & (\tilde{\mathbf{Y}}(0))_{3,2} & (\tilde{\mathbf{Y}}(0))_{3,3} & (\tilde{\mathbf{Y}}(0))_{3,4} \\ -N_{11}(L) & -N_{12}(L) & 0 & 0 & 0 & 0 \\ 0 & 0 & (\tilde{\mathbf{Y}}(L))_{4,1} & (\tilde{\mathbf{Y}}(L))_{4,2} & (\tilde{\mathbf{Y}}(L))_{4,3} & (\tilde{\mathbf{Y}}(L))_{4,4} \\ 0 & 0 & -(\tilde{\mathbf{Y}}(L))_{3,1} & -(\tilde{\mathbf{Y}}(L))_{3,2} & -(\tilde{\mathbf{Y}}(L))_{3,3} & -(\tilde{\mathbf{Y}}(L))_{3,4} \end{bmatrix} \quad (\text{B.4})$$

In Eqs.(B.3)-(B.4), $(\tilde{\mathbf{Y}}(\cdot))_{i,j}$ denote the (i,j) element of matrix $\tilde{\mathbf{Y}}(x)$ in Eq.(19). From Eqs.(B.1)-(B.2) the following nodal matrix relation can be derived

$$\mathbf{f} = \mathbf{\Xi} \mathbf{\Gamma}^{-1} (\mathbf{u} - \mathbf{u}^{(f)}) + \mathbf{f}^{(f)} = \mathbf{D}(\omega) \mathbf{u} + \mathbf{f}_0 \quad (\text{B.5})$$

where

$$\mathbf{D}(\omega) = \mathbf{\Xi} \mathbf{\Gamma}^{-1} \quad (\text{B.6})$$

$$\mathbf{f}_0 = -\mathbf{\Xi} \mathbf{\Gamma}^{-1} \mathbf{u}^{(f)} + \mathbf{f}^{(f)} \quad (\text{B.7})$$

In Eqs.(B.6)-(B.7), $\mathbf{D}(\omega)$ and \mathbf{q} are the exact dynamic stiffness matrix and exact load vector of the beam in Fig. 1. Numerical applications of this paper show that Eq.(B.6) coincides with Eq.(31), while Eq.(B.7) coincide with Eq.(36). Upon deriving the nodal displacements, the frequency response in every member is computed from Eq.(18), where the vector of integration constants is back calculated from the nodal displacements using the following expression

$$\mathbf{b} = (\mathbf{\Gamma})^{-1} (\mathbf{u} - \mathbf{u}^{(f)}) \quad (\text{B.8})$$